Abstract

DASH, GORDON H. Investigation of a Combined Heat and Power Fuel Cell System for Small Scale Residential Applications. (Under the direction of Dr. Richard Johnson)

Fuel cell technology is an emerging technology that provides a highly efficient, quit operation, and environmentally friendly energy conversion technology for stationary and mobile applications. Stationary fuel cell applications have received greater attention for their ability to capture the heat rejected, from the production of electricity, for heating applications. This paper evaluates a modeled PEMFC system, and presents the heat and power efficiencies of the system. The method used to evaluate the system is the TRNSYS simulation. TRNSYS models the transient performance of thermal systems by using a modular structure.

A model of the PEMFC system is developed to determine the energy required to meet the hourly average electric load of the residence. The model evaluates the amount of heat generated and the amount of heat used for thermal loads of the residence. The electricity for lights, appliances, and space cooling is provided by the PEMFC, the space heating and water heating is provided by the thermal energy generated from the PEMFC, which is stored within two hot water storage tanks. An electric resistance heater, and an electric water heater will supplement the space heating and water-heating load not provided by the PEMFC.

The results of this research show that a 1.5KW system, with a heat exchanger UA value of 5239 kJ/hr-K, and main storage and hot water tank sizes of 80 and 40 gallons, will provide up to 40% energy savings over conventional systems. The system will provided up to 65% cogeneration efficiencies. The economics of the system show that the price of the PEMFC system with a reformer needs to be priced at $20/cell.

Investigation of a Combined Heat and Power Fuel Cell System for Small Scale Residential Applications

By:

Gordon H. Dash III

A Thesis Submitted as Partial Fulfillment
of the Requirements for the Degree of

MASTER OF SCIENCE
MECHANICAL ENGINEERING

NORTH CAROLINA STATE UNIVERSITY

2003

Approved By:

Dr. Herbert Eckerlin

Dr. Nancy Ma

Dr. Richard Johnson
Chairman Advisor Committee

Biography

Gordon H Dash III was born in Providence, RI on April 20, 1979. He attended Classical High School where he excelled as a long distance track runner. In the Fall of 1997 he enrolled at North Carolina A&T State University in Greensboro NC, where he majored in Civil Engineering. While attending NC A&T he was able to run track, maintain various part time jobs, and excel in his school work. It was at NC A&T where he developed his love for energy efficient and renewable energy systems. He received his Bachelor of Science Degree in Civil Engineering in May 2001.

After earning his B.S. Degree he was awarded a gradate scholarship from the Graduate of Engineering Minorities. With this scholarship he entered college in the Fall of 2001 at North Carolina State University in Raleigh, NC, where he has pursed his Master of Science Degree in Mechanical Engineering.

Table of Contents

List of Tables

List of Figures

Chapter 1: Introduction:

The U.S. accounts for 25% of the world's total energy consumption. In 2000, the U.S. consisted of 102 million households, where 73% are single-family households; using 10 quadrillion BTU's of energy. The households spent a total of 136 billion dollars on energy, of which 88 billion dollars and 3.5 quadrillion BTU's of energy were in the form of electricity. Electricity is an important role in the everyday life of society. Electricity is used to power many household items, one-third of the electricity loads are used to power appliances, refrigerators, and lights, and the other two-thirds is used for space heating, cooling, and hot water loads. It is seen that electricity is one of the most important energy sources for daily life, unfortunately it is extremely expensive, and the production is very harmful to the earth. Electricity is produced from the burning of fossil fuels. This large-scale production can achieve approximately 40% efficiency, but the burning of fossil fuels leads to an extreme amount of environmental waste, of greenhouse gases into the earth's atmosphere. With alarming environmental issues the government is trying to find ways to reduce the environmental impacts the U.S. is creating for the world. The government is looking for environmental friendly ways for producing energy.

Green powered energy is energy that is not strictly renewable but it is environmentally friendly because the results of the produced energy do limited harm to the environment. A combined heat and power system [CHP] produces on site electricity, while also producing thermal energy that may be utilized for space and water heating applications. A CHP system utilizing a fuel cell is very attractive for residential applications because the thermal energy produced is almost equivalent to the amount of electricity generated. The generated thermal and electrical energy are produced with high efficiencies, quite operation, and low environmental impacts.

There are many design considerations involved with the development of fuel cell systems; three possible designs are represented in Figures 1,2 and 3. Design option one includes a natural gas fuel cell system to supply the lights, appliances, and electric space cooling loads of the residence. The space heating loads will be supplied by a water-to-air heat exchanger. Design option one allows for a very small fuel cell system, and minimum equipment requirements. Because the fuel cell stack is an expensive component of the system, the overall price may be lower than the following designs.

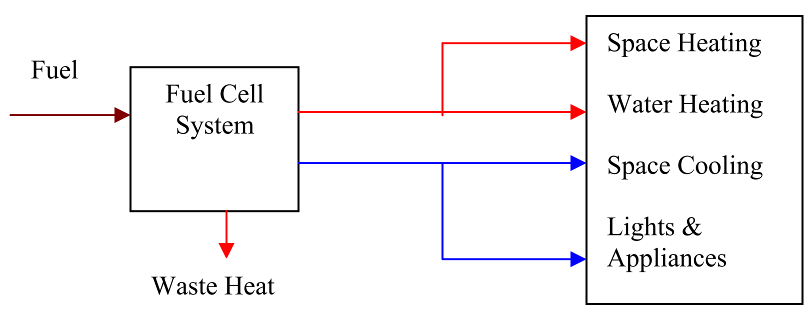

Figure 1.1 Fuel Cell Systems with Heat Recovery for Thermal Heating

The second design consists of the fuel cell system being sized to supply the electricity for all of the loads in the residence. The system will consist of a vapor compression heat pump that will supply the space cooling and a minimum amount of space heating loads. The waste heat generated will supply the water heating and additional space heating

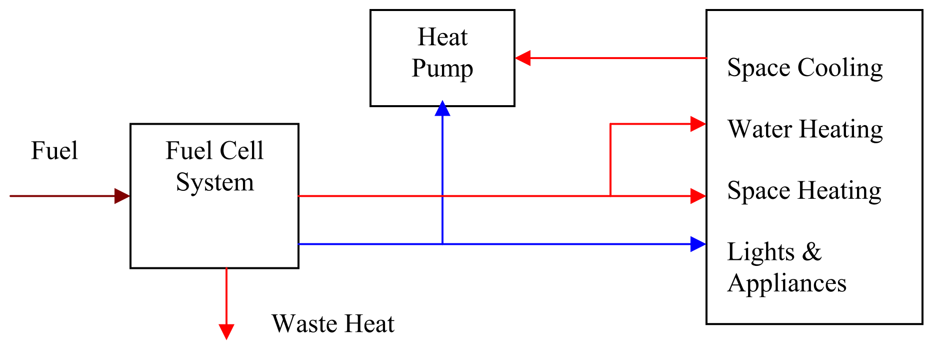

Figure 1.2 Fuel Cell Systems with Heat Pump Recovery System

The third design will not require natural gas for the fuel cell, which will not require a reformer in the fuel cell system, and will lead to higher performance rates. There will be photovoltaic system providing enough electricity to operate an electrolyser. The electrolyser will create hydrogen from the disassociation of water molecules. The hydrogen will be stored in a tank and will supply the fuel cell with pure hydrogen. This design consideration is very expensive due to the fact the, production of hydrogen from electrolysis id very energy intensive and will not produce hydrogen at very high efficiency ratings, therefore reducing the overall efficiency of the system.

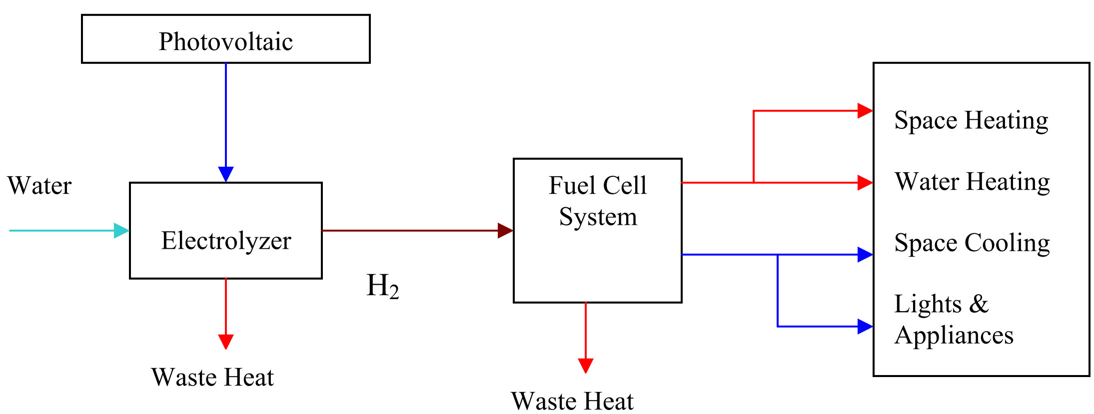

Figure 1.3 Photovoltaic Powered Fuel Cell System

This research will look at design option one, for the fact that it will require a very small fuel cell system, which will power the base loads of the lights appliances and space cooling. The heat generated will be stored to provide the space heating and water heating loads of the residence.

Chapter 2: Problem Statement

The objectives for this research are to determine the feasibility of implementing a combined heat and power fuel cell system for various climatic regions of the country. This research will look at the residential energy requirements for a single family detached dwelling, model the performance of a combined heat and power fuel cell system in response to the energy requirements, and to evaluate the life cycle savings for the combined heat and power system compared to conventional all electric and natural gas and electric systems.

The residence design calculations for this research will be designed based on typical single family detached dwellings for specific climatic regions. The size and the characteristics of the house are based on data from the Energy Information Administration (EIA) [1] and other documented sources within this literature. The residences will all be based on four-person occupancy; all the design characteristics are based on current residential building codes, the space heating and cooling loads will be supplied within the TNSYS simulation model. [2]

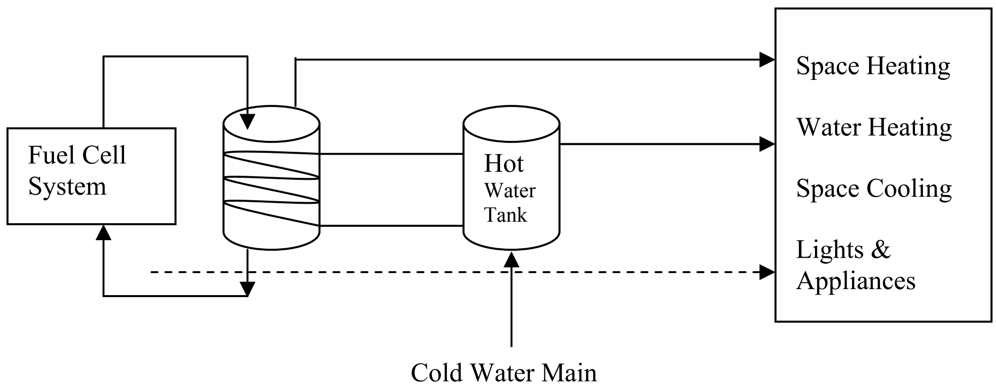

Figure 2.1 Combined Heat and Power Fuel Cell System

The combined heat and power [CHP] fuel cell system as shown in Figure 2.1 is different from conventional systems because the thermal heat generated from electricity can be used for domestic water heating, space heating, and fuel processing. The CHP system will operate by supplying electricity to the lights, appliances, and space cooling loads. The thermal energy from the fuel cell system is transferred to a thermal storage tank via a heat exchanger. The thermal storage tank will distribute the thermal energy to the water and space heating needs. The model will look at the energy savings for the system; optimize the size and flow rates for the heat exchanger, and optimize the size of the thermal storage tanks.

Chapter 3 Review of Literature

3.1 Residential Energy Requirements

The United States consumed 98.50 quadrillion BTU's of energy in the year 2000 and the consumption is projected to increase to 130.9 BTU's by the year 2020, an annual increase of about 1.4% The residential sector consumed 10.25 quadrillion BTU's of energy for the year

2000 of which 8.46 quadrillion BTU's was consumed by single family houses. The residential consumption is projected to grow at an average rate of 1% per year until 2020, giving a total residential energy requirement of 24.3 quadrillion BTU's. The energy requirements for a single-family residential application will consist of energy for lights, appliances, domestic hot water, space heating and space cooling. Figure 3.1 shows the projection of the various energy requirements for the residential market. It can be seen that space heating and water heating are the two largest consumers of energy in the residential market. The energy requirements for the residential energy consumption will vary with climatic conditions; therefore this research will study for different climatic areas of the country, and the affect on residential energy consumption. Figure 3.2 shows the breakdown of various climatic zones as specified by the EIA, and Table 3.1 shows the chosen cities for the research.

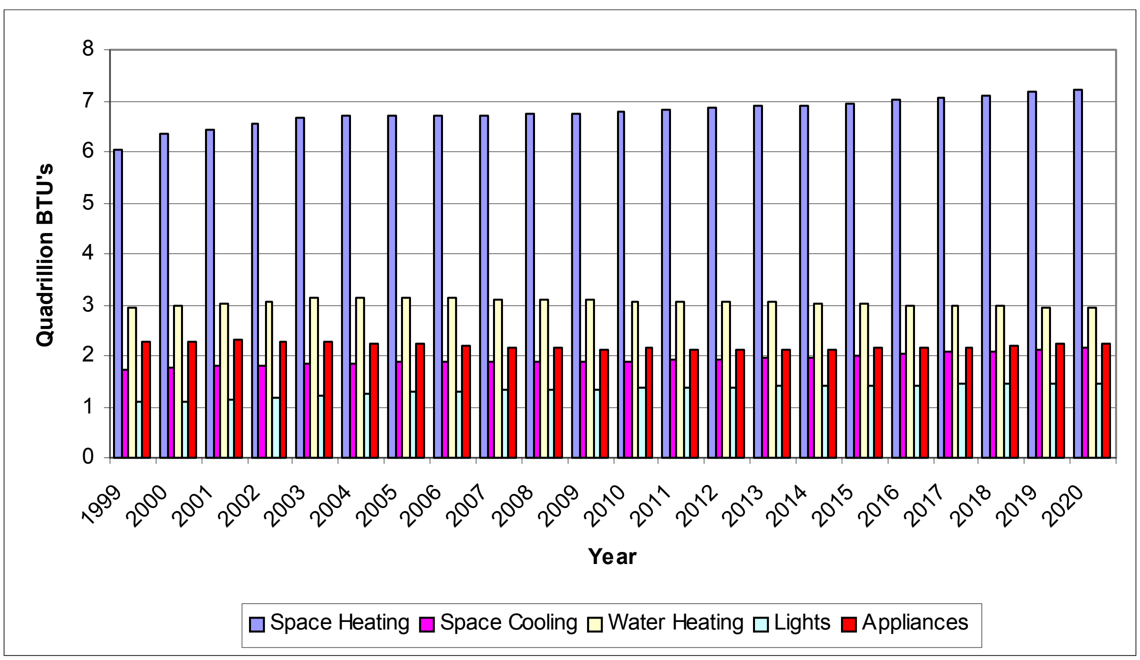

Figure 3.1 Residential Energy Projections

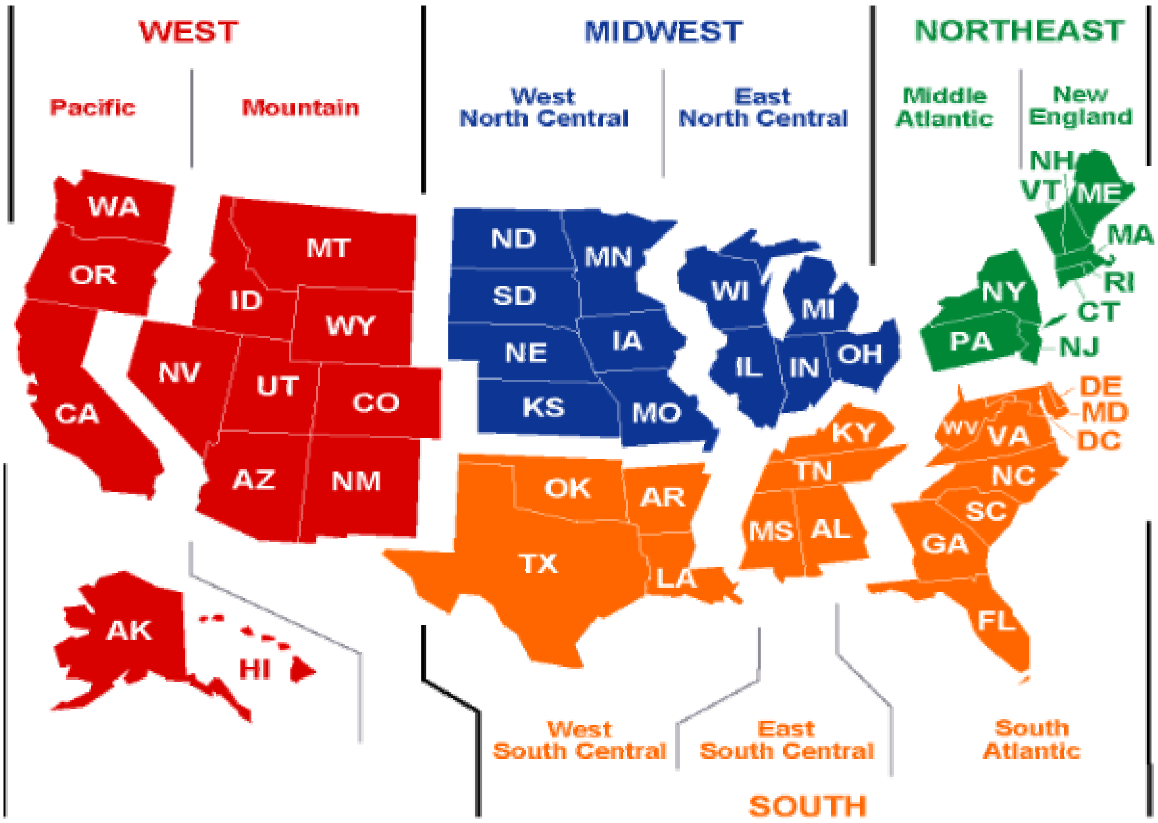

Figure 3.2 EIA Climatic Regions

Northeast	Boston, Massachusetts
South	Atlanta, Georgia
Midwest	Chicago, Illinois
West	Sacramento, California

Table 3.1 Chosen Cities For Research

3.2 Combined Heat and Power Systems

A combined heat and power system, otherwise known, as a cogeneration system is the simultaneous production of electricity and heat using a single fuel. The heat from the production of electricity can either be used for domestic or industrial purposes, creating efficiencies upward to 90% or more. [3] The advantages of having a fuel cell cogeneration system are greater efficiencies of energy conversion than conventional ways of producing electricity, possible reduction in harmful emissions, such as the main greenhouse gas CO_2, and the opportunity to move towards decentralized forms of electricity generation. Decentralized systems may limit the risk of customers being left without heat or power, and may provide the added benefit of cost savings. Presently CHP systems supply 8% of the U.S. electric power, reduce NO_x and SO_2 emissions by 0.9 and 0.4 million tons per year respectively, reduce 35 million metric tons of carbon equivalent in the atmosphere, and CHP systems save over $5 billion per year in fuel costs. [4]

Cogeneration consists of four basic elements; prime mover, electricity generator, heat recovery, and control system. The cogeneration unit is typically named after the prime mover, generator and fuel used. The main cogeneration systems used are steam turbines, gas turbines, combined cycle turbines, fuel cells, and micro-turbines. Steam turbines expand high-pressure steam from a boiler within a turbine to produce mechanical energy used to run an electric generator. Steam turbines are classified according to the exit pressure of the steam, either as backpressure turbines, where the exit pressure is greater than atmospheric, or as condensing turbines where the exit pressure is lower than atmospheric, requiring a condenser. The basic schematics of the backpressure and condensing turbines are seen in Figure 3.3.

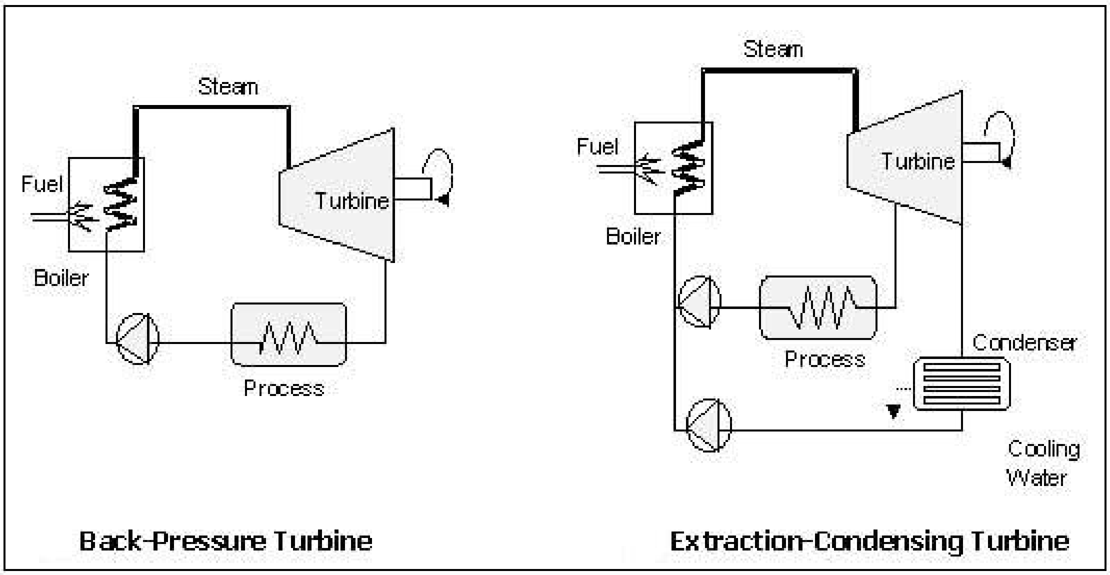

Figure 3.3 Schematic of Steam Turbines in Cogeneration Systems

Gas Turbine technology has experienced a rapid development in recent years due to the greater availability of natural gas, reduced capital costs, improved reliability, and enhanced environmental reductions. Mechanical energy is created when fuel is burnt and passed through a gas turbine as seen in Figure 3.4. The mechanical energy will most commonly be used to produce electricity with a generator, or it may be used to drive pumps, compressors, blowers, etc. Natural gas is the most commonly used fuel, because natural gas has the minimum amount of contaminants, which could cause corrosion under the high temperature and high-speed operations. The exhaust gas can be used in many different ways, either for direct firing and drying process, to raise steam at medium or low pressure for process or space heating, and also to generate high temperature hot water. Gas turbines will also drastically reduce the amount of NO_x formation; by reducing the combustion temperature. The reduction in combustion temperature is achieved by steam injection, which will also increase the turbine electrical generation efficiency.

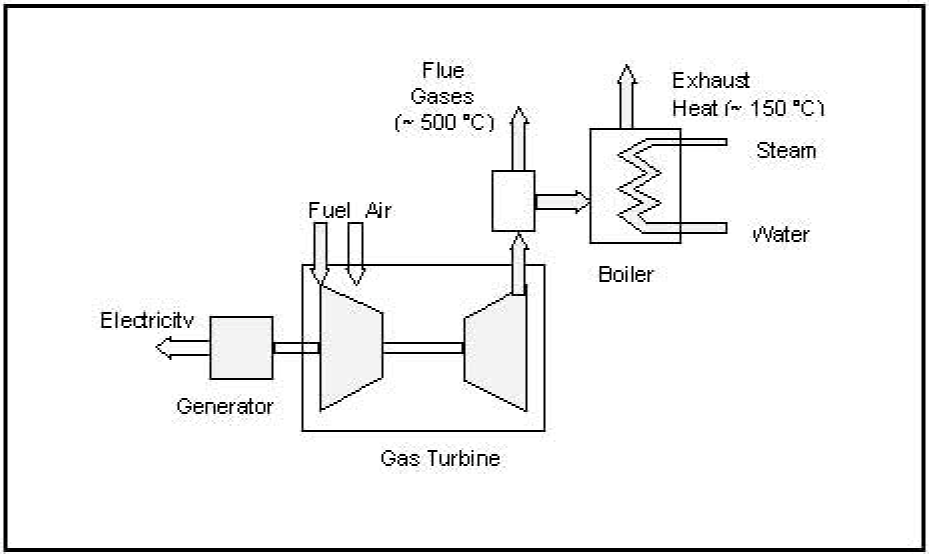

Figure 3.4 Schematic of a Gas Turbine in Cogeneration Applications

Combined-cycle systems utilize the technology of gas turbines, with a steam turbine. The hot exhaust gases from the gas turbine system are raised to a temperature to produce steam and the steam is used run a turbine producing greater electrical efficiencies.

Micro turbines are essentially a miniature gas turbine system. They are high-speed generator power plants that include a turbine, compressor, generator, which are all on a single shaft. Micro turbines have great opportunities in the generation of using waste and biogas, residential applications, and for the backup power.

Fuel cells operate on the conversion of chemical energy, and do not require mechanical work. Fuel cells provide high efficiencies, low emissions, and reliable operation. The basics of fuel cell systems will be described in the following section.

3.3 Fuel Cells

A fuel cell is an electrochemical system where the chemical energy of a fuel is converted directly into electrical energy and heat with the aid of an oxidant. Fuel cells have received more attention in the past few years due to their very low emissions, quiet operation, modular designs, cogeneration applications, rapid load response, and high efficiency rates. Since fuel cells are electrochemical the conversion of the chemical energy takes place by charge separation. Analyzing the fuel cell itself, there are three main components, anode, cathode, and electrolyte. The anode is the negative side of the fuel cell. The anode is where the fuel, usually in the form of a gas, is feed to the fuel cell. The fuel used is mainly hydrogen. Hydrogen may be extracted from many different hydrocarbon gases such as natural gas. The hydrogen gas ionizes and releases electrons and creates H^+ ions:

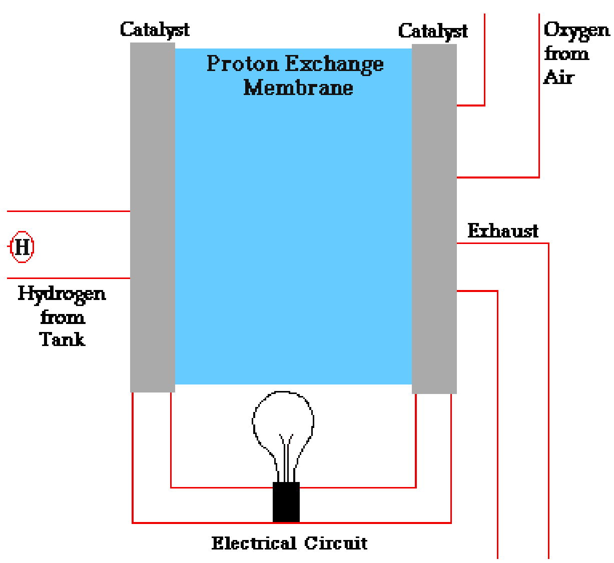

Figure 3.5 Operation of a Fuel Cell

$$2H_2 \rightarrow 4H^+ + 4e^- \quad (3.1)$$

The cathode is the positive side of the fuel cell; this is where the oxidant, mainly oxygen, is fed and reacts with the electrons and brings the electrons back to the catalysts where they combine with the H^+ ions to form water:

$$O_2 + 4e^- + 4H^+ \rightarrow 2H_2O \qquad (3.2)$$

The electrolyte is used to transfer the H^+ ions from the cathode to the anode. The different types of electrolytes used are what characterize the specific name of the fuel cell. Table 3.2 gives a brief description of the type of fuel cell electrolytes used and their operating temperatures.

Type	Electrolyte	Operating Temp. [C]
Alkaline	Potassium Hydroxide	50-90
Proton Exchange membrane	Polymeric	50-125
Direct Methanol	Sulfuric Acid or Polymer	50-120
Phosphoric Acid	Orthophospheric Acid	190-210
Molten Carbonate	Lithium/Potassium carbonate mixture	630-350
Solid Oxide	Stabilized Zircona	900-1000

Table 3.2 Type of Fuel Cell Electrolytes

3.3.1 Thermodynamics of Fuel Cells

The second law of thermodynamics applied to fuel cells has many advantages over conventional systems in many ways. [5] One way is that the electrochemical combustion of fuel is able to avoid irreversibilities, where conventional systems have many conversion steps for converting fuel's chemical energy into electricity. The avoidance of irreversibilities is possible because whenever there is fuel oxidation the fuels valence electrons move toward lower energy states, which are the products of the combustion reaction. A conventional combustion process will use the lowering of energy states in direct heating of combustion products. In a fuel cell, or electrochemical reaction, part of the released energy can be taken directly as electricity by taking the valence electrons before the final reduction reaction and to move the electrons through a conductor attached to an external circuit. When looking at an electrochemical reaction on a macroscopic level [6], we will notice ions will pass through an electrolyte, the ions will drop in potential and the ions will also carry a power with them, which will be distributed as electricity though an external load. At the end of the process the final oxidation reaction is less dissipative than a conventional combustion process therefore making fuel cells more superior than conventional systems. Fuel cells also add an advantage to the second law of thermodynamics when combined with a conventional energy system. Looking at a conventional system, the closer the first topping cycle's use of released heat is to the maximum combustion temperature, the more use can be made of chemical energy in the fuel. Fuel cells avoid this reasoning because they use the direct conversion of a fuels chemical energy into work followed by the release of heat at a temperature within the range of conventional systems. A second advantage of a combination of a conventional system and a fuel cell is there will be a reduction in the irreversibility's in a conventional combustion process. The reduced irreversibility's are credited for two reasons; the first is the fuel can reform the exhausts gases from the bottoming cycle of the conventional system. The second reason is in the combustion process of a conventional system, the partial combustion needed in a fuel cell is completed in the bottoming cycle of the conventional system.

When considering the thermodynamics and efficiency of a fuel cell, there are three main properties to consider: Gibbs-free energy, Helmholtz function, and enthalpy. The Gibbs-free energy is the energy available to do external work, neglecting any work done by the changes in pressure and/or volume. The external work in fuel cells is the moving of electrons around an external circuit. All of our thermodynamic properties are dependent upon the Gibbs-free energy. The energy released is determined by the Gibbs free energy of formation:

$$\Delta G = G\ (of\ Products) - G\ (of\ reactants) \tag{3.3}$$

We know that the Gibbs-free energy of formation changes with temperature and state. If we assume that that the fuel cell works isothermally, and the state does not change, then from the second law of thermodynamics for a reversible process:

$$\Delta Q_{rev} = T\Delta S = \Delta H - \Delta G \tag{3.4}$$

ΔQ_{rev} = change in thermal energy

T= Temperature

ΔS = Entropy change

ΔH= Enthalpy change

ΔG =Gibbs-free energy

We have made the assumption that the fuel cell is reversible (no losses in the fuel cell) this means that all of the Gibbs-free energy will be converted to electrical energy. [7] This assumption will allow us to find the electromotive force or the reversible open circuit voltage. The electrical work done is equal to the product of the charge and voltage and with the reversible assumption and definition of Gibbs-free energy all of the electrical work will be the Gibbs-free energy:

$$\Delta G = -zFE \tag{3.5}$$

z=number of electrons per molecule in the electrochemical reaction

F= Faraday number

E= Voltage of the Fuel Cell

Solving for the reversible open circuit voltage:

$$E=-\Delta G_f/zF \tag{3.6}$$

The maximum efficiency possible for an operating is determined by:

$$\eta = \frac{\Delta \bar{g}_f}{\Delta \bar{h}_f} * 100\% \tag{3.7}$$

The assumption of having no losses in the fuel cell has determined the maximum theoretical efficiency for fuel cells, but it has been proven that an operational fuel cell will not produce the predicted value. There will be losses in the actual voltage of a fuel cell due to: activation losses, pressure and gas concentrations, and ohmic losses. Activation losses are determined by how ions are discharged to and from the electrodes. When the electrons are released and the charged fuel ion combines with the electrolyte ion to form a product, energy is required for this process, which means there will be a voltage drop. The voltage drop may be found from experimental work conducted by Tafel in 1905, where he studied the overvoltage at the surface of an electrode, the results of his work produced the equation known as the Tafel equation:

$$V = E - A * Ln\left(\frac{i}{i_o}\right) \tag{3.8}$$

E= Reversible Open Circuit Voltage (Equation 3.6)

A= Theoretical Constant

i= Operating Current Density

i_o = Exchange Current Density

The second limiting factor is the pressure and gas concentrations, which is the loss of potential due to the inability of surrounding material to maintain initial concentration of the bulk fluid. There are two types of concentration losses; the first is the reduction of potential due to the change in concentration of electrolyte in the area of the electrode during the reaction. The second concentration loss is due to the changes in concentration of the reactant gas in the area of the reaction zone at the electrode. These losses are determined by the Nernst equation [8]:

$$E = E^o + \frac{RT}{2F} Ln\left[\frac{a_{H2O} \cdot a_{O2}^{1/2}}{a_{H2O}}\right] \tag{3.9}$$

Where a is the activity which is equal to the partial pressure of the gas divided by the standard pressure, E^0 is the reversible open circuit voltage at standard pressure, and R is the universal gas constant. The third limiting factor is the resistance polarization, which is a cause a potential loss when there is a change in the specific conductivity of the electrolyte.

$$V = ir \tag{3.10}$$

Where i is the current density and r is the specific area resistance. The actual voltage of a fuel cell may now be determined by equation 3.11

$$V = E - E_{act} - E_{ohmic} \tag{3.11}$$

Where E may be determined by equation 3.9, E_{act} and E_{ohmic} may be determined from equation 3.8 and 3.10 respectively. The fuel cell efficiency may now be determined by equation 3.12

$$\eta = \frac{V}{E^o} \tag{3.12}$$

The typical operation of a PEM fuel cell operating at 70 C is depicted in Figure 3.6 [7].

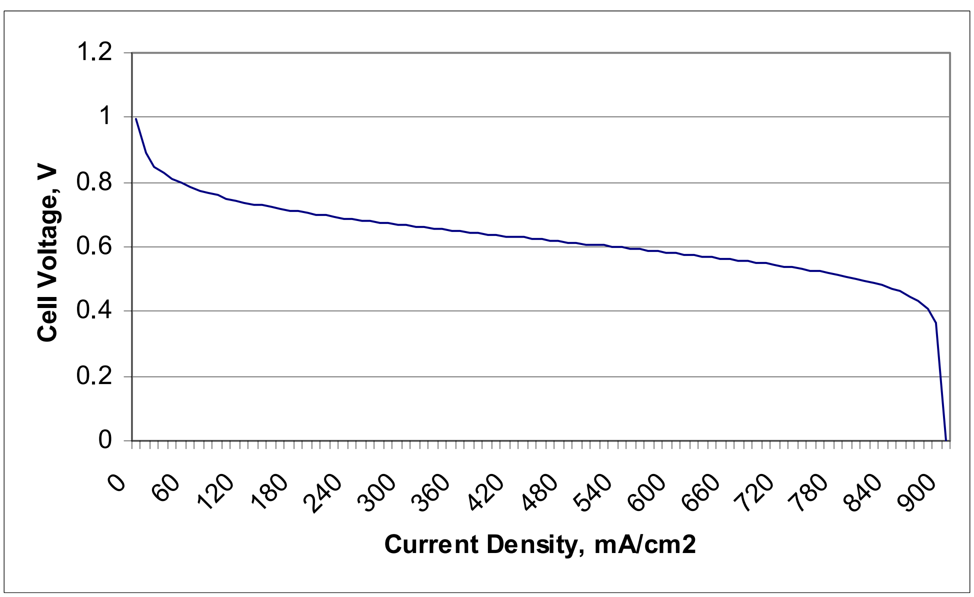

Figure 3.6 Fuel Cell Operating at 70

It can be seen that the open circuit voltage is less than the theoretical no loss value, there is a rapid drop off in current density initially, the voltage is rather linear from 200 to 800 current density, and there is a rapid drop off in voltage at very high currents. Figure 3.6 proves that fuel cells will operate at a higher voltage with lower loads.

3.4 Residential Application Studies on Fuel Cell Systems

Gunes [8] has studied a PEM fuel cell system to meet residential heating and power demands. Gunes looked recovering the thermal heat dissipated from the fuel cell stack, and utilizing for water heating and additional space heating, while the large portion of the space-heating requirement would be meet by a heat pump, which will also supply the residence with the required space cooling. Gunes concluded that a fuel cell system with an output of 4 kWhe and 5 kWhe would provide 78% cogeneration applications for southern and northern climates respectively. Krist [9] conducted a study on the design and application SOFC for residential applications, and concluded that a system of 1kW would be an optimal size based on thermal-to-electric loads of the residence. Bos [10] studied the commercialization and marketing of fuel cell systems and suggests that a system will be optimized at 2 kW; Bos did not take into consideration system sizing considerations, cogeneration applications, or operating strategies. Braun [11] studied a SOFC system with a dual storage tank, and modeled the system from 1kW to 10kW size range. Based on the residential applications Braun found that for a single family detached dwelling a SOFC system will be optimized at 1kW.

Chapter 4 Analysis

In this chapter the models required to simulate the components needed for the combined heat and power system are described. In order to accurately determine the performance of the CHP system the energy requirements for the specified components are specified. The program TRNSYS mathematically connects the components of the CHP system and links them to the required residential energy requirements.

A schematic of the CHP system is shown in Figure 4.1, with the main components consisting of a PEM fuel cell system, thermal storage system, heat exchanger, auxiliary heating and cooling, and various controls and sensors. Detailed models for all the components are presented in this chapter.

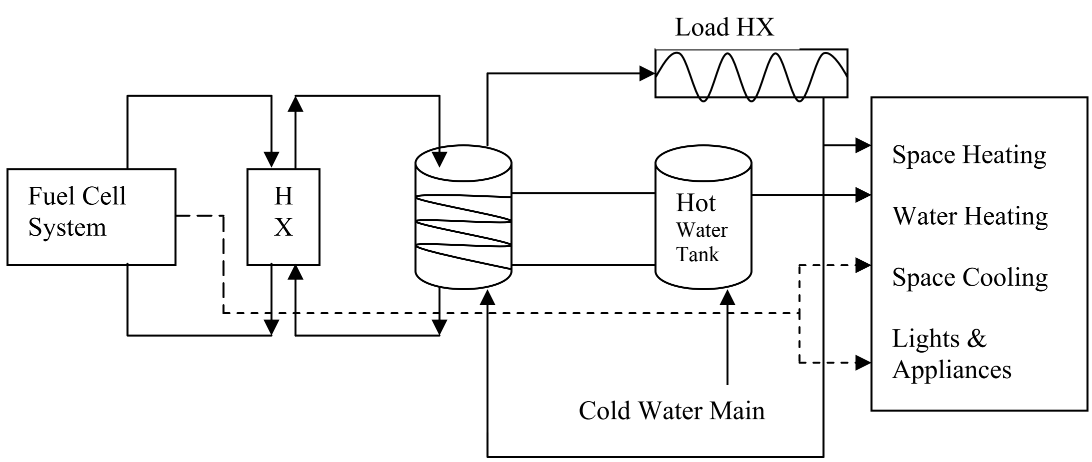

Figure 4.1 Schematic of Combined Heat and Power System

4.1 TRNSYS

TRNSYS is a transient system simulation program with modular structure. It is designed to simulate the transient performance of thermal systems. A thermal system is considered to be a connection of separate thermal components all connected in a way to perform a specified task. The modular structure of the TRNSYS system is a collection of components all with a specified FORTRAN subroutine evaluating the components performance, based on specified parameters, input, outputs, and time dependent forcing functions. The output is the information flowing out of the component; the input is the information flowing into the component and is the outputs of another component. The parameters will not change throughout the simulation; they model the FORTRAN subroutine of the component. The time dependent forcing functions form another set of inputs that change with time, but are not outputs of another component. An example of a forcing function is the hot water usage profile that change every hour but is dependent on human behavior. The components in TRNSYS will be identified by a specified TYPE number, with each type number relating to a specified FORTRAN subroutine coded to that number. For example TYPE 3 would model a pump in TRNSYS. There may be cases where there will be more than one TYPE number associated in the system simulation and in order to organize the system a UNIT number will be assigned to the specified TYPE. The Unit number is designed to be a reference number and have no performance relation to the TYPE number.

4.2 Simulation Input

4.2.1 Weather Data

In order to perform a transient simulation on a thermal system, hourly weather data must be provided. The preferred weather data for simulation program is TMY2 data. TMY2 data is a set of hourly values of measured or modeled solar radiation and meteorological data for 239 stations for the 30-year period from 1961-1990. The data is statistically constructed to develop a typical one-year solar radiation and meteorological data; since the data is constructed to represent a typical year it cannot be used to determine performance on a worse case condition. The data was developed for computer simulations to determine the performance of different systems for different locations in the United States.

4.2.2 User Data

The daily, monthly, and hourly user loads depend on the type of household, characteristics of household occupants, and the climatic region. One of the goals of this research is to determine typical user input for various climatic regions. The user loads will consist of determining the typical hot water load profiles, typical thermal properties of single-family houses, and typical electrical usage for a single-family residence. The user data will be modeled as a time dependent forcing function.

4.3 Residential Energy Requirements

Residential energy is required for domestic water heating, space heating, space cooling, and electricity for lights and appliances. The proposed CHP system will supply electricity for the lights and appliances and also for space cooling with an electric air conditioner, the thermal energy dissipated from the CHP system will supply the required amount for space heating and water heating. The thermal energy for space heating will be supplemented with auxiliary heating for times when the CHP system cannot supply the required heating needs, and the hot water needs will be supplemented with an auxiliary heater for times the thermal energy from the CHP system is not adequate enough. The characteristics for each energy demand shall be discussed below.

4.3.1 Domestic Hot Water

Domestic hot water is the second largest consumer of thermal energy in the residential sector, second to space heating. To determine the appropriate hot water energy usage, the hourly consumption water profiles, incoming city water temperature, the temperature of the hot water source, and seasonal variation are all contributing factors. The difficulty in determining the correct hot water energy usage lies within specific parameters, which cannot be accurately determined on a wide scale basis; such factors are number and type of occupants in the household, and the hot water equipment. This section will determine a typical hot water profile. The domestic hot water characteristics will be based on a two-story single-family residence with four occupants (2 children and 2 adults), dishwasher, clothes washer, 2 showers and one bathtub. This research has studied four hot water consumption databases, and analyzed each study to develop an accurate hourly consumption profile for a typical single-family residence. The first study was conducted by, Becker and Stogsdill [13] They researched nine published articles on hot water daily and hourly consumption profiles, and they aggregated these studies and developed a database that gives an accurate hot water profile for single-family residence. The second study was conducted by, Lowerstein and Hiller [14. They found that field data for hot water profiles was very complex and expensive; they developed an inexpensive and very accurate way to measure hot water consumption. They used thermocouples on individual hot water branch lines (flow signature), to determine the individual hot water draws. Their case study involved 12 different residential houses. The third study produced by Aquacraft, Inc [15] used a flow trace analysis to determine the percentage of a specific hot water category on an hourly basis as seen in Figure 4.2

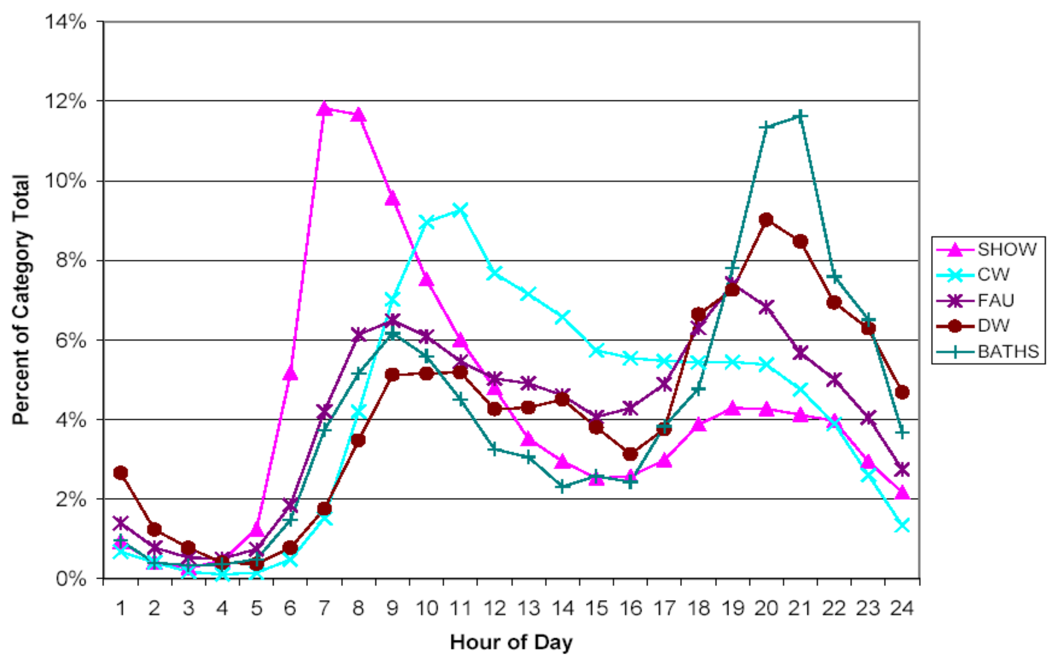

Figure 4.2 Percentage of Hot Water on an Hourly Basis

A comparison of the percentage of hourly hot water category and the average consumption per category will give an accurate determination of the hourly consumption of hot water. Table 4.1 depicts the average water draw for a particular category.

Table 4.1 Average Water Draw for Water Endues

Category	Per Capita (gcd)	House Use (gal/day)	Percent of total Hot Water use	Percent of overall use that is hot water
Bath	4.2	10.9	16.7	78.2
Clothes Washer	3.9	10.1	15.5	27.8
Dishwasher	0.9	2.3	3.6	100
Faucet	8.6	22.4	34.3	72.7
Leak	1.2	3.1	4.8	26.8
Shower	6.3	16.4	25.1	73.1
Toilet	0	0	0	0
Other	0.01	0.03	0	35.1
Total	25.1	65.3	100%	39.60%

The fourth study analyzed was published in the ASHRAE handbook of fundamentals [16]. A comparison of the four hourly consumption profiles is shown in Figure 4.3

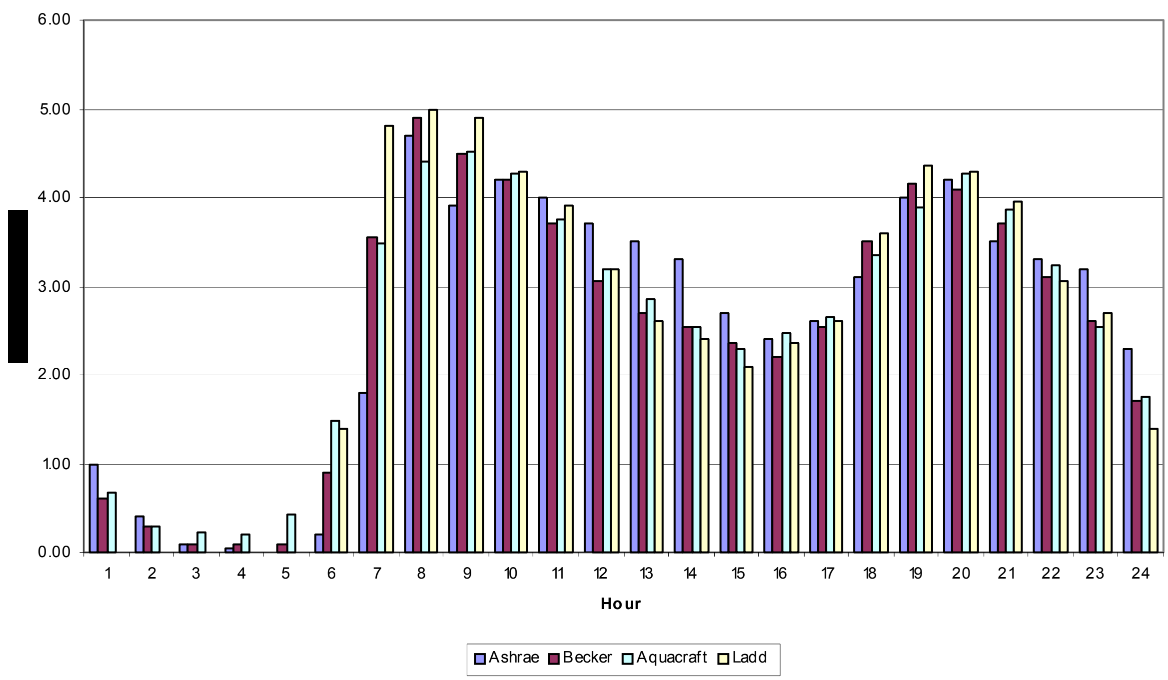

Figure 4.3 Comparison of Hourly Hot Water Draws

The average daily consumption of hot water from the four hourly test results is 63.23gal/day. The seasonal variation will also have an affect on the performance of the hot water profile; Figure 4.4 shows a representation presented by Becker of a typical consumption variation on a monthly basis.

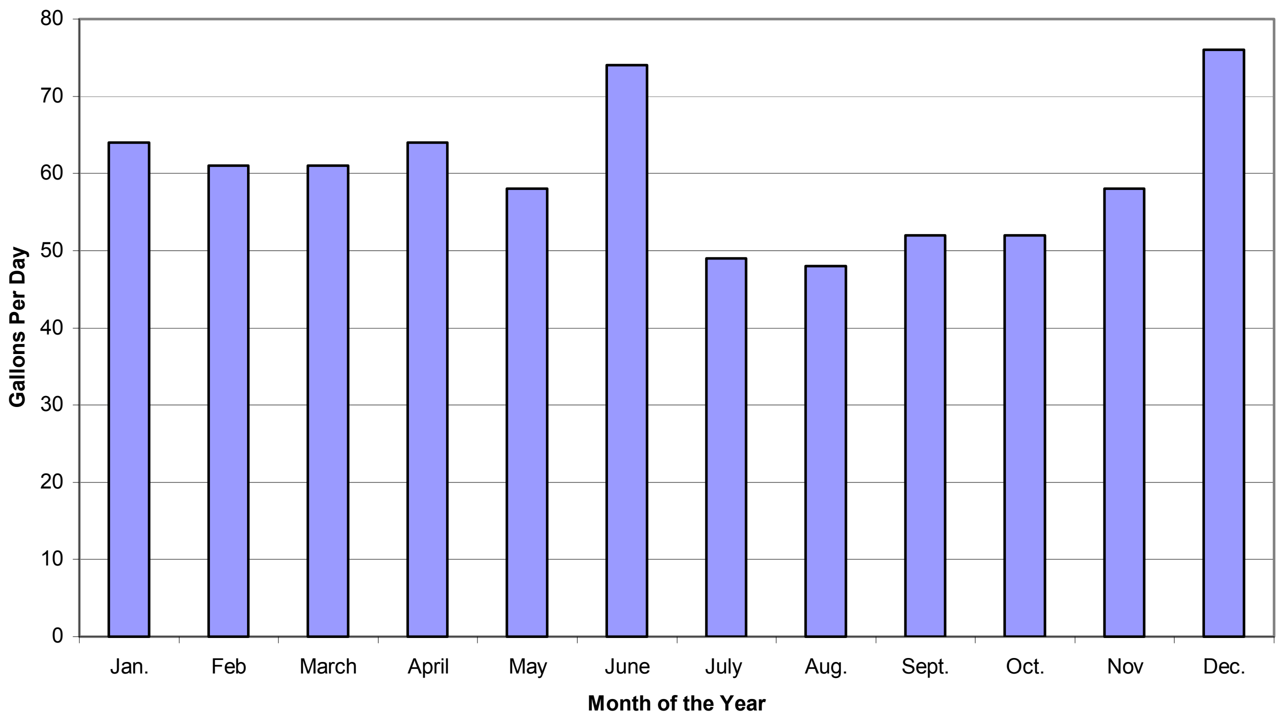

Figure 4.4 Hot Water Consumption Seasonal Variation

A comparison of the average daily consumption and the seasonal variation will yield the hot water energy use that will be used in the research, which is shown in tabular and graphical format in Table 4.2.

Hour	Jan.	Feb.	March	April	May	June	July	August	Sept.	October	Nov.	Dec.
1	6.13	5.89	5.89	6.13	5.66	6.13	4.94	4.86	5.18	5.18	5.66	7.07
2	5.52	5.28	5.28	5.52	5.04	5.52	4.33	4.25	4.57	4.57	5.04	6.46
3	5.25	5.01	5.01	5.25	4.77	5.25	4.07	3.99	4.30	4.30	4.77	6.19
4	5.21	4.97	4.97	5.21	4.74	5.21	4.03	3.95	4.27	4.27	4.74	6.16
5	5.29	5.05	5.05	5.29	4.82	5.29	4.11	4.03	4.35	4.35	4.82	6.24
6	6.93	6.70	6.70	6.93	6.46	6.93	5.75	5.67	5.98	5.98	6.46	7.88
7	11.50	11.26	11.26	11.50	11.02	11.50	10.32	10.24	10.55	10.55	11.02	12.44
8	14.04	13.81	13.81	14.04	13.57	14.04	12.86	12.78	13.09	13.09	13.57	14.99
9	13.48	13.25	13.25	13.48	13.01	13.48	12.30	12.22	12.53	12.53	13.01	14.43
10	13.07	12.84	12.84	13.07	12.60	13.07	11.89	11.81	12.12	12.12	12.60	14.02
11	12.32	12.08	12.08	12.32	11.84	12.32	11.13	11.05	11.37	11.37	11.84	13.26
12	11.27	11.03	11.03	11.27	10.79	11.27	10.08	10.00	10.32	10.32	10.79	12.21
13	10.56	10.32	10.32	10.56	10.09	10.56	9.38	9.30	9.61	9.61	10.09	11.51
14	10.15	9.92	9.92	10.15	9.68	10.15	8.97	8.89	9.21	9.21	9.68	11.10
15	9.52	9.28	9.28	9.52	9.05	9.52	8.34	8.26	8.57	8.57	9.05	10.47
16	9.51	9.27	9.27	9.51	9.03	9.51	8.32	8.24	8.56	8.56	9.03	10.45
17	9.97	9.74	9.74	9.97	9.50	9.97	8.79	8.71	9.03	9.03	9.50	10.92
18	11.46	11.22	11.22	11.46	10.99	11.46	10.28	10.20	10.51	10.51	10.99	12.40
19	12.80	12.56	12.56	12.80	12.33	12.80	11.62	11.54	11.86	11.86	12.33	13.75
20	13.03	12.79	12.79	13.03	12.55	13.03	11.84	11.76	12.08	12.08	12.55	13.97
21	12.15	11.92	11.92	12.15	11.68	12.15	10.97	10.89	11.21	11.21	11.68	13.10
22	11.05	10.81	10.81	11.05	10.58	11.05	9.87	9.79	10.11	10.11	10.58	12.00
23	10.27	10.04	10.04	10.27	9.80	10.27	9.09	9.01	9.33	9.33	9.80	11.22
24	8.43	8.20	8.20	8.43	7.96	8.43	7.25	7.17	7.49	7.49	7.96	9.38

Table 4.2 Hot Water Hourly Energy Use [kg/hr]

The required hot water temperature will be dedicated to 60 C, as specified by ASHRAE. The incoming water temperature is the last parameter in determining the residential hot water demand; a study conducted by the Controlled Energy Corporation [17] details the incoming city water temperatures for various climatic regions. Table 4.3 summarizes the average city water residential inlet water temperature.

	January	February	March	April	May	June
Boston, MA	12.38	11.82	11.90	12.38	13.85	15.31
Atlanta, GA	14.85	14.28	14.22	14.50	15.61	16.72
Chicago, IL	14.08	13.00	12.90	13.43	15.49	17.54
Sacramento, Ca	13.18	11.63	11.51	12.24	15.18	18.13
	July	**August**	**September**	**October**	**November**	**December**
Boston, MA	16.60	17.46	17.67	17.21	16.24	15.08
Atlanta, GA	17.69	18.29	18.35	17.85	16.92	15.85
Chicago, IL	19.35	20.47	20.56	19.65	17.90	15.90
Sacramento, Ca	20.64	22.26	22.39	21.08	18.60	15.76

Table 4.3 Averaged Monthly City Inlet Water Temperature [C]

4.3.2 Space Heating & Cooling

The requirements for space heating and cooling loads will be determined and evaluated by using a Type 12 component within the TRNSYS program. The Type 12 component models heating and cooling loads through a single conductance (UA) for heat loss or gain, along with any additional gains due to lights, people, etc. A single energy balance on the house is performed for each simulation time step. The room temperature and the heat loss from the building will be evaluated by the equations 4.1 and 4.2:

$$Q_L = UA\left(\overline{T}_R - T_a\right) - Q_{gain} \tag{4.2}$$

The room temperature is allowed to float between the set temperature points for heating and cooling, if the room rises above the maximum temperature or falls below the minimum temperature then, the energy required to maintain the required temperature is the output as the cooling or heating requirement. The heating of the room is maintained through a load heat exchanger and auxiliary heater, while the cooling of the room is maintained by air conditioning. ASHRAE suggests that the heating room temperature is set at 21C, while the cooling room temperature is set at 25C. The load heat exchanger will be modeled specifying the product of the effectiveness of the water-air heat exchanger and the minimum fluid capacitance rate, where Duffie and Beckman [18] suggest a value twice the UA value of the household will provide an effective an economical load heat exchanger size. The rate of which energy is transferred into the space across the load heat exchanger will be determined by equation 4.2:

$$Q_T = \gamma \varepsilon C_{\min} \left(T_i = \overline{T}_R \right) \tag{4.3}$$

When the load heat exchanger cannot provide the adequate heating for the residence an electric resistance heater will be activated, and the rate of auxiliary energy provided to the residence is determined by equation 4.4

$$Q_{aux} = Q_L - Q_T + \frac{CAP\left(T_{RF} - T_{RL} \right)}{\Delta t} \tag{4.4}$$

4.3.2.1 House Conductance

The overall thermal conductance of the house is dependent upon the building size, material characteristics, infiltration, geographic location, and internal gains (lights, occupancy). The dimensions of single-family houses are developed in many different shapes and sizes; the Lawrence Berkeley National Laboratory [19] has conducted research on a typical single-family house sizes for various geographic regions. The house dimensions are broken into two regions: North and South. The North region will simulate the housing dimensions for Chicago and Boston, while the south region will simulate the housing dimensions for Atlanta and Sacramento. Table 4.4 provides the dimensions for different housing types for each region respectively.

Table 4.4 Residential Building Dimensions								
	North Region				South Region			
Housing Type	Small Single Family	Large Single Family	Muti family	Manufactured Homes	Small Single Family	Large Single Family	Muti family	Manufactured Homes
Number of Stories	1	2	1	1	1	1	1	1
Foundation Type	Unheated Basement				Slab			
Component Dimensions (Square feet)								
Conditioned Floor Area	1227	2892	1074	1207	1336	2562	1056	1195
Ceiling	1227	1446	479	1207	1336	2562	490	1195
Walls	1002	2349	476	993	1051	1785	480	987
Windows	147	347	73	145	160	307	48	143
Infiltration	1227	2892	1074	1207	1336	2562	1056	1195
Foundation Area	1227	1446	31	1207	1336	2562	31	1195
Foundation Perimeter (feet)	144	169		142	151	262		141

Table 4.4 Residential Building Dimensions

The typical home in each region will be used for the research, and in this case the large single family housing dimensions will be analyzed, it should be noted that for the northern regions two stories will be used while for the southern regions one story houses will be analyzed. The floor areas for the two housing units have been sized according to typical new home construction sizing, and the wall height will be assumed to be 8ft.

The National Fenestration Rating Council [20] has conducted research on the typical regional single-family homes foundation and the homes material thermal resistance. Table 4.5 provides the various building properties with the given thermal capacitance values for each.

Table 4.5 Thermal Resistance Values						
	Ceiling	**Wall**	**Floor**	**Slab**	**Basement**	**Window**
	R value $hr\text{-}ft^2$ F/Btu (m^2 C/W)	R value $hr\text{-}ft^2$ F/Btu (m^2 C/W)	R value $hr\text{-}ft^2$ F/Btu (m^2 C/W)	R value $hr\text{-}ft^2$ F/Btu (m^2 C/W)	R value $hr\text{-}ft^2$ F/Btu (m^2 C/W)	U Value $Btu/hr\text{-}ft^2$ ($W/m^2\text{-}C$)
Boston	38 (6.7)	19 (3.3)	--	--	11 (1.9)	0.40 (2.3)
Chicago	38 (6.7)	19 (3.3)	--	--	14 (2.5)	0.40 (2.3)
Atlanta	38 (6.7)	19 (3.3)	13 (2.3)	2 (0.4)	--	0.65 (3.7)
Sacramento	26 (4.6)	11 (1.9)	11 (1.9)	0	--	0.70 (4.0)

Table 4.5 Thermal Resistance Values

Infiltration is referred as the rate of uncontrolled air exchange through unintentional openings that occur under given conditions. The infiltration rate depends on weather conditions, occupant activity, and air leakage, where air leakage is the measure of the tightness of a building. The infiltration rate, expressed as air exchanges per hour (ACH), and air leakage may be expressed by the following equation:

$$ACH = L\,(0.006 * \Delta T + 0.03U^{1.5}) \qquad (4.8)$$

Where L is the air leakage, U is the wind speed and ΔT is the indoor to outdoor temperature difference. The structure considered in this research will be a medium tight and will have a value of 3 for air leakage per month. Figure 4.5 gives the average ACH for each month, and it may be seen that the seasonal variation can have a tremendous difference on the rate of air exchange, ranging from 0.9 in January to 0.33 in July for Boston.

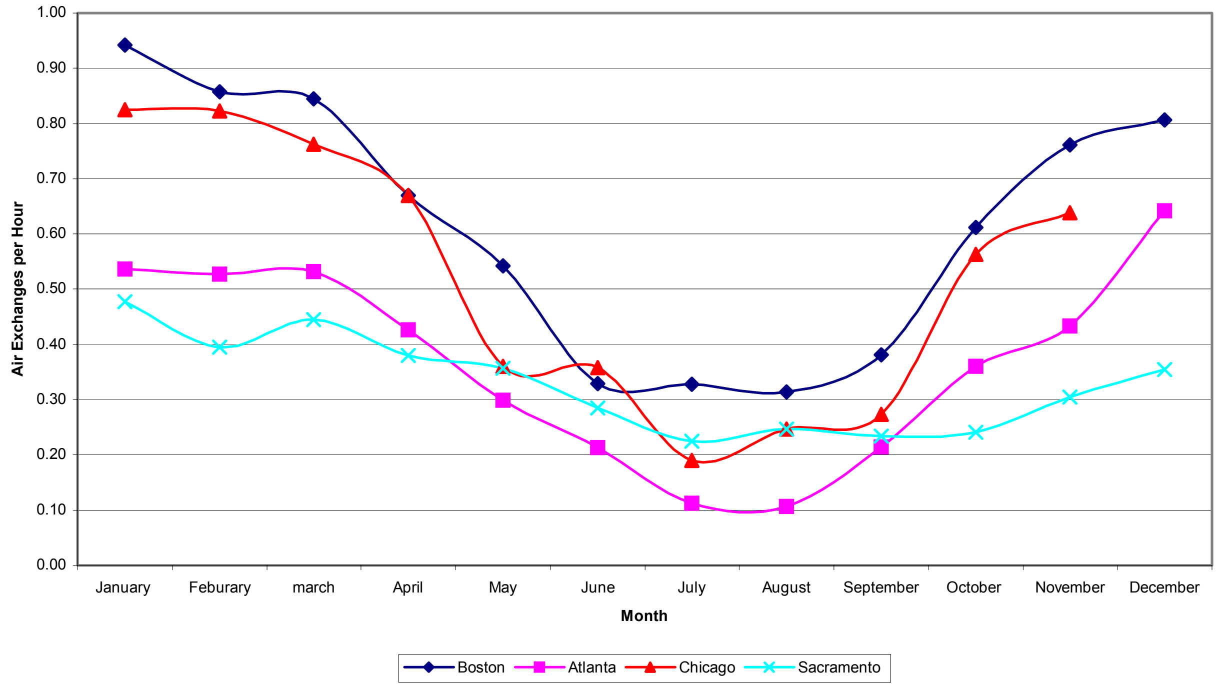

Figure 4.5 Variations of Air Exchanges per Hour with Month

The internal gains will include energy from the lights, appliances, and number of occupants. ASHRAE recommends that and estimate of 67 W per person is sufficient in determining the internal loads within a single-family residence, therefore a total of

965 kJ/hr will be used for the internal gains.

Analyzing the building size with the thermal resistance calculations, and adding the comparison of the volume of the house with the average ACH from Figure 4.5 may determine the average overall conductance of the house. The house conductance for the four regions vary, Figure 4.6, the southern climates is relatively consistent throughout the year, while the northern climate house conduction varies considerable during the winter months, this is due to the colder ambient conditions, and high wind velocities. The average UA value for each region may also be found on Figure 4.6

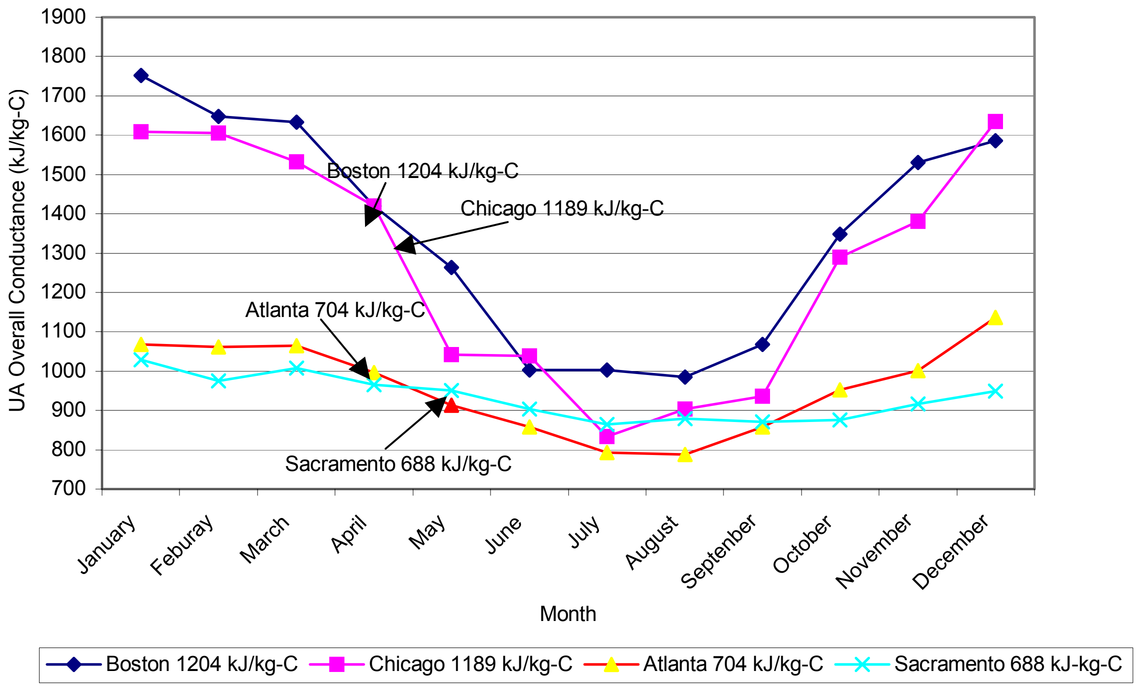

Figure 4.6 Monthly Average House Conductances

4.3.3 Electric Loads for Lights and Appliances

Data for lights and appliances has been determined from the National Association of Home builders (NAHB). A recent survey conducted by the NAHB [21] will be used for the data on electric loads. The report uses annual data from the Residential Energy Consumption Survey (RECS), monthly data from builders, hourly profiles from three utility companies, and detailed energy use from field measurements. The hourly electrical data included within the report was complied from three companies; Southern California Edison Territory, Baltimore Gas & Electric, and Public Service Electric & Gas Territory. The average, median, maximum, and minimum electrical consumption are shown for each hour of the year for a typical single-family home, according to the EIA, in Figure 4.7 through Figure 4.11.

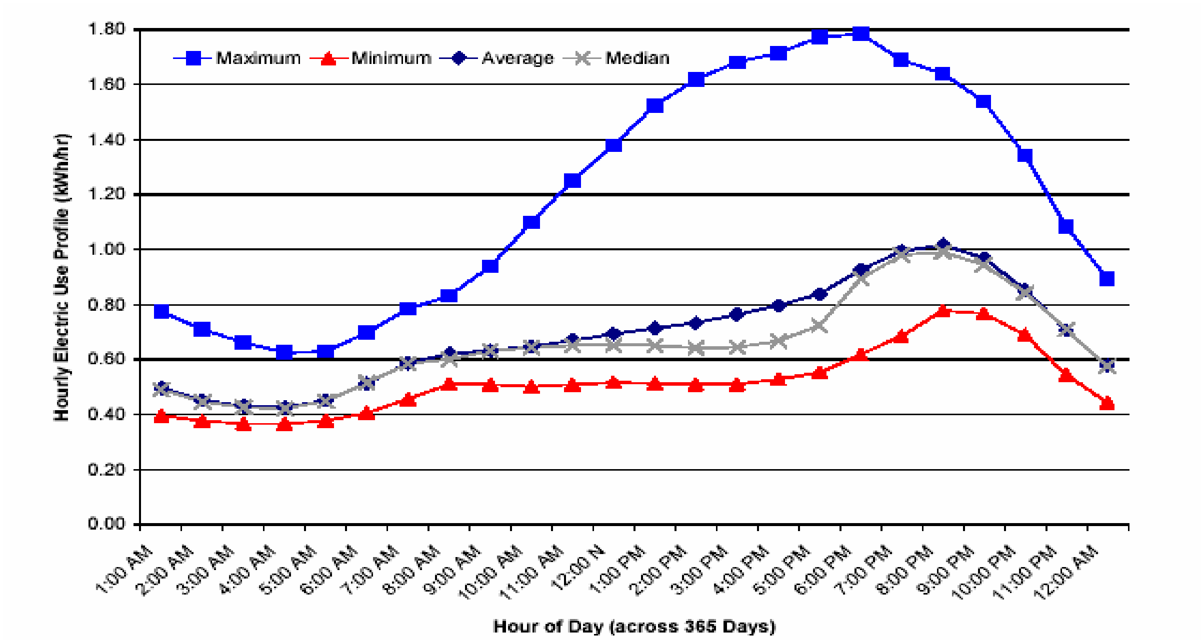

Figure 4.7 Hourly Load Profile (Southern California Edison Territory)

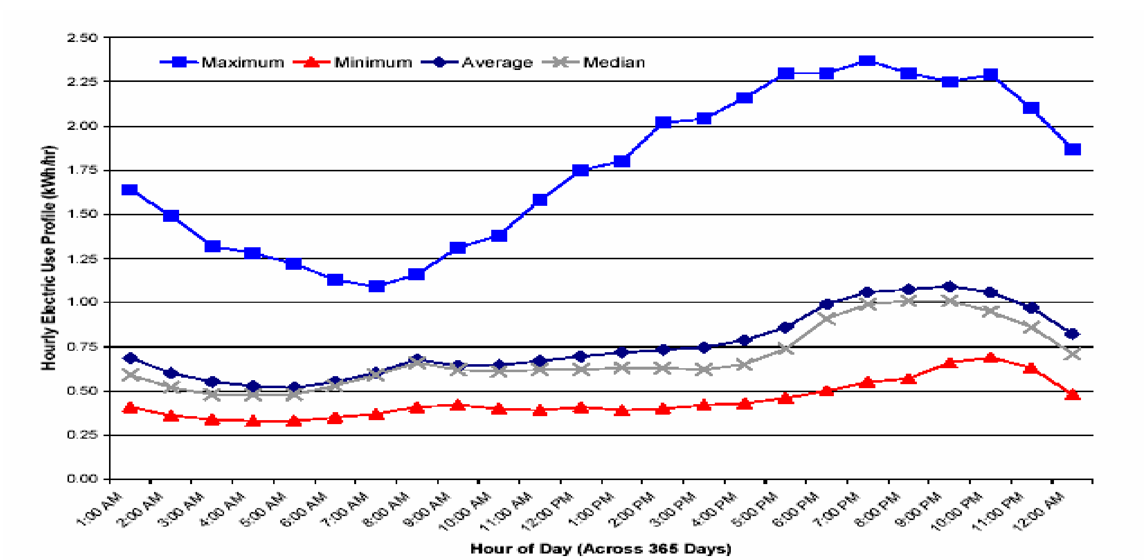

Figure 4.8 Hourly Load Profile (Public Service and Gas Territory) Non-Electric Space Heating

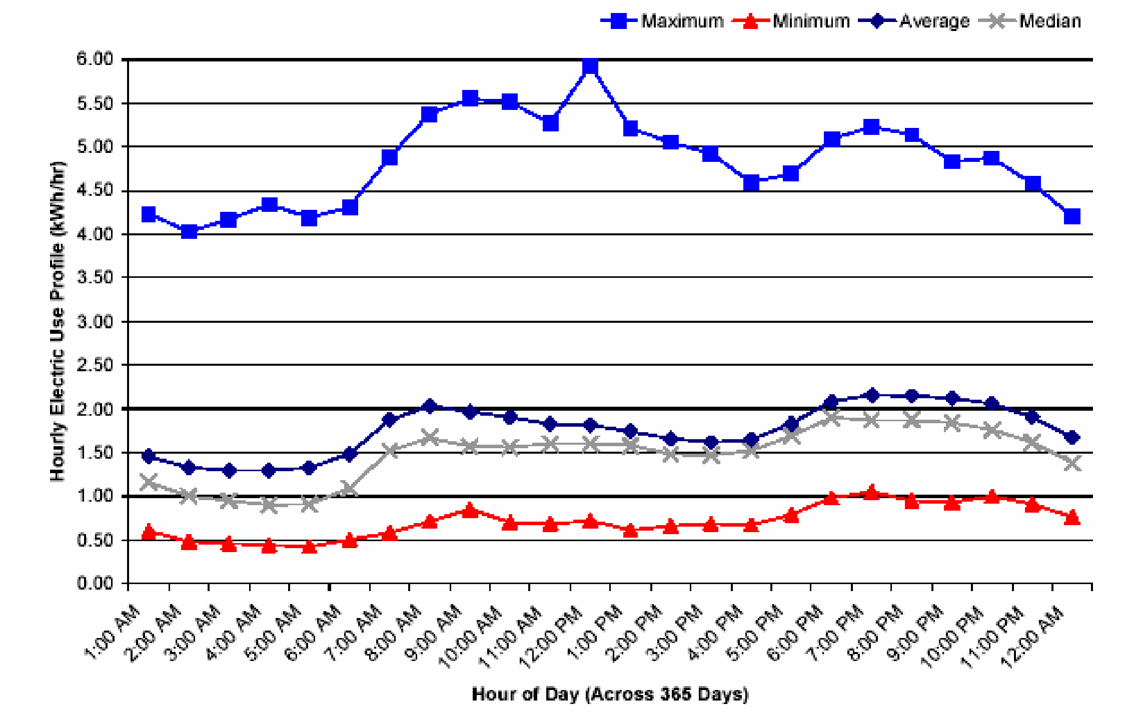

Figure 4.9 Hourly Load Profile (PSGT) Electric Space Heating

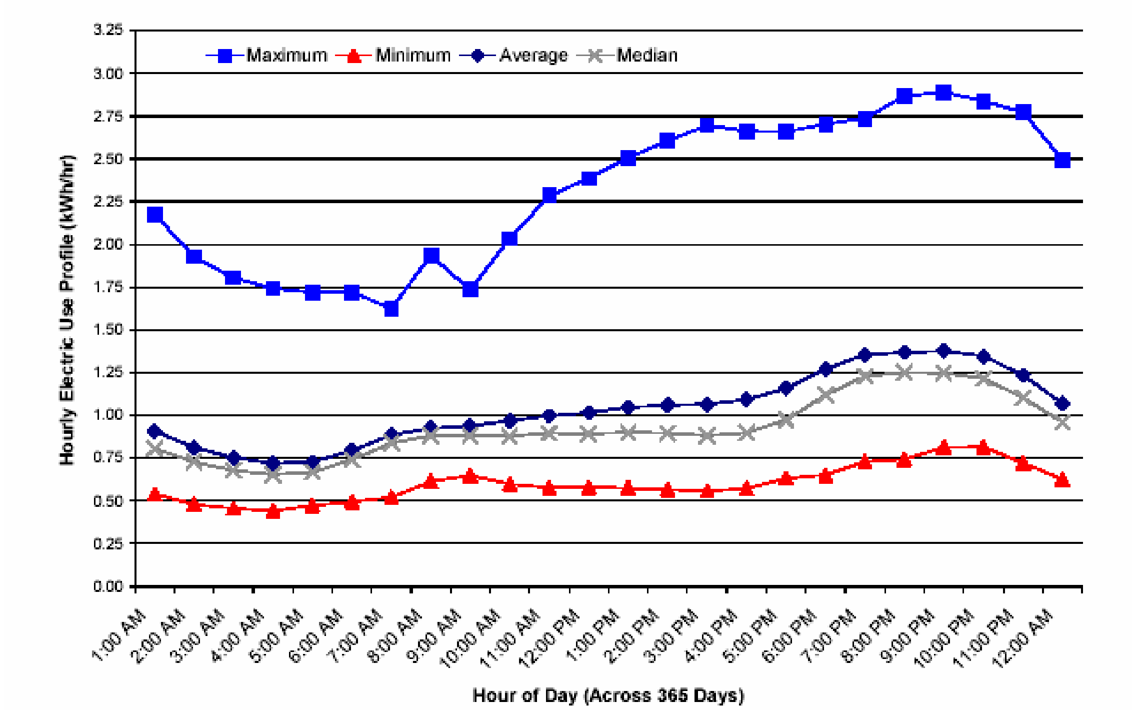

Figure 4.10 Hourly Load Profile (Baltimore Gas and Electric Territory) Non-Electric Space Heating

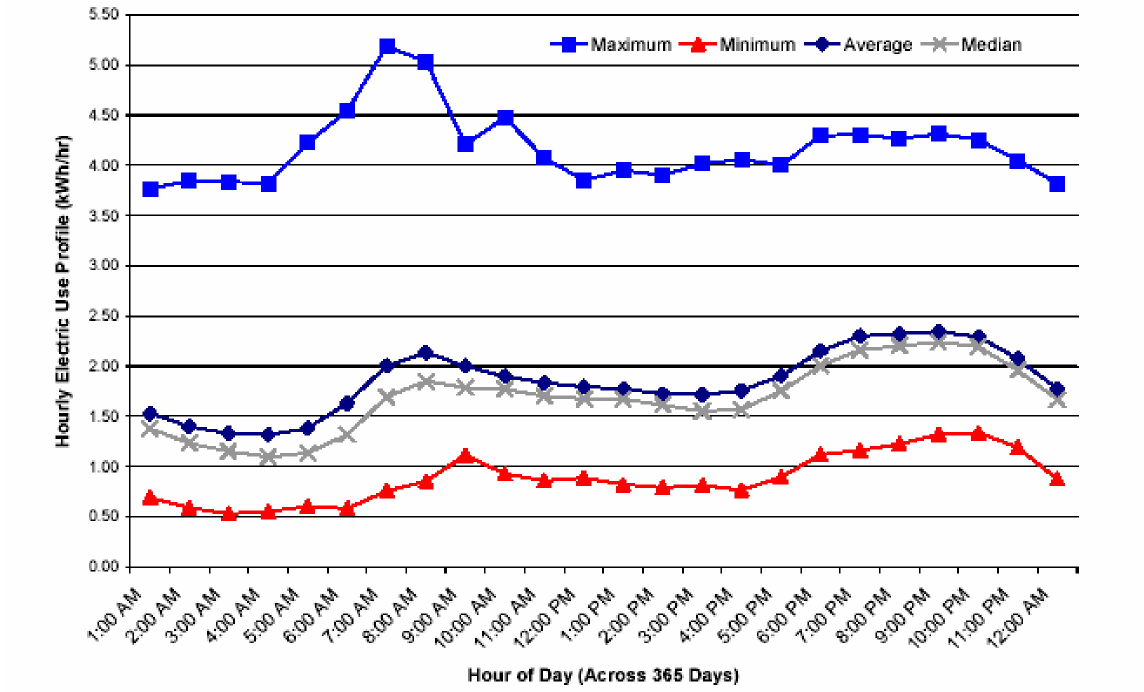

Figure 4.11 Hourly Load Profile (BGET) Electric Space Heating

The hourly load profiles for each of the three utility companies have been developed to represent a typical electrical daily demand, for a typical single family home within the companies' specific region. The hourly electric consumption is shown to be fairly consistent for the three utility companies, there is a comparative difference between the maximum and average values compared to the minimum and average values, the average values will be used in determining the typical electrical hourly demand. Comparing the hourly profiles and averaging the totals will determine the profile used for the TRNSYS simulation.

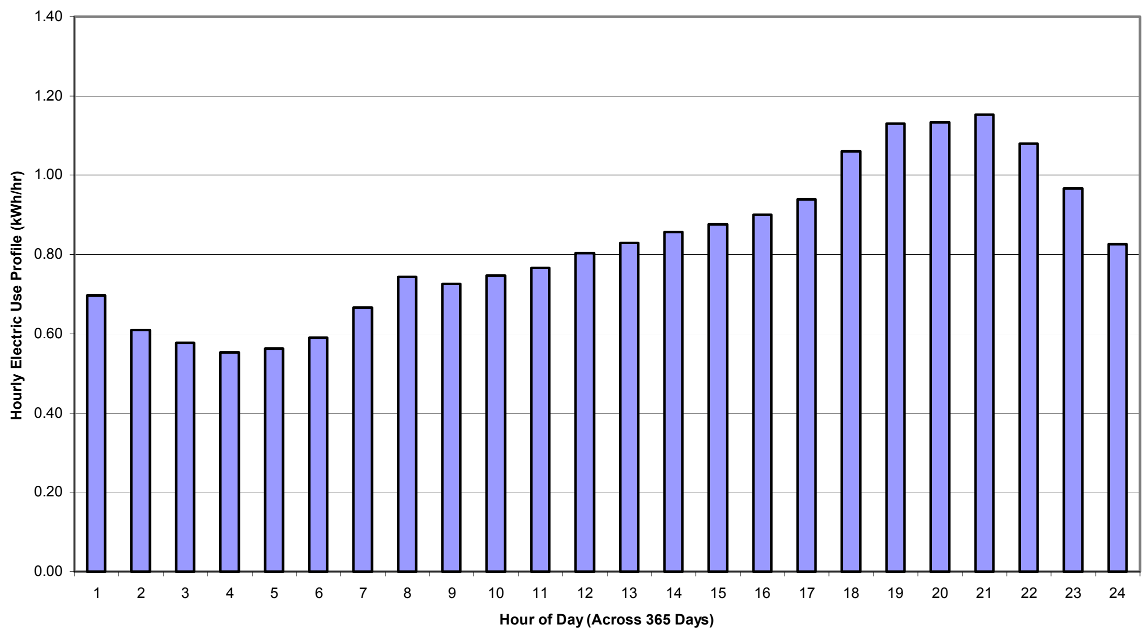

Figure 4.12 Hourly Electric Load Profile

Figure 4.12 depicts the hourly electric load profile for the typical design characteristics for this research. The maximum electric load for the residence with non-electric space heating is 1.15 kW. The amount of electric space heating will vary for various climatic regions of the country, but this profile will give an estimate of the amount of electric consumption provided by the fuel cell system for lights and appliances.

The data presented above is data for the average electric consumption for an hour in a single-family residence. The actual peak electric loads will not be reflected in the previous profiles, because the fuel cell is not designed to handle short transient durations of loads, and it is also not economically feasible to design a fuel cell for the maximum peak electric loads. In order to compensate for this situation a battery pack is introduced to the system, and the battery pack will be designed to handle the transient effects.

The capacity and peak output of the battery pack can be determined by investigating the electricity demand of the residence on a short-term basis. The research conducted by the

NAHB provides the analysis of a home studied for a period of one year. Figure 4.13 provides the 15-minute demand data of the presented study.

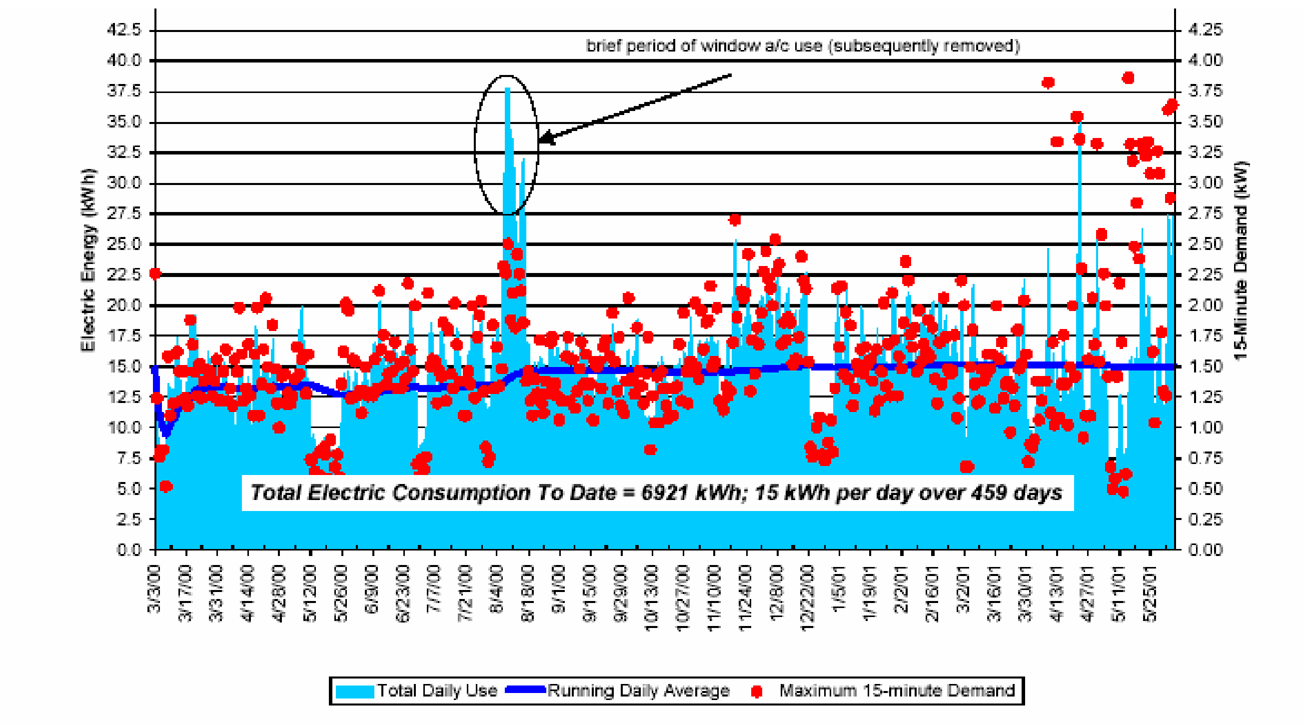

Figure 4.13 15-Minute Electrical Demands

The research provided that on a 15-minute interval the maximum demand of the home is 4.0 kW, and on a 1-minute interval the maximum demand is 5.1 kW. The minimum demand for a 15-minute interval has been determined to be 0.12 kW and for a 1-minute interval 0.0 kW. The battery pack must be sized to handle the peak power electrical demand of the residence, and must also have a sufficient storage capacity for times when the fuel cell system cannot supply the required electrical demand. According to Figure 4.13, the peak power electrical requirement is 25 kW, while the minimum power requirement is 0.5 kW. Assuming that the minimum requirement of the residence occurs for 8-hours, the battery will need to have a storage capacity of 4kWh.

4.3.4 Representative Residential Energy Requirements

The following section represents the monthly residential energy requirements for each city. It is shown that the monthly space heating loads are higher in the winter months, for the colder climates, and the space heating loads are higher for the warmer climates. The difference in the heat loads will have an effect on the thermal storage tanks, because more thermal energy will be demanded in the winter months for the colder climates, than for the warmer climates. This created a larger amount of excess heat dissipated into the atmosphere for the colder climates.

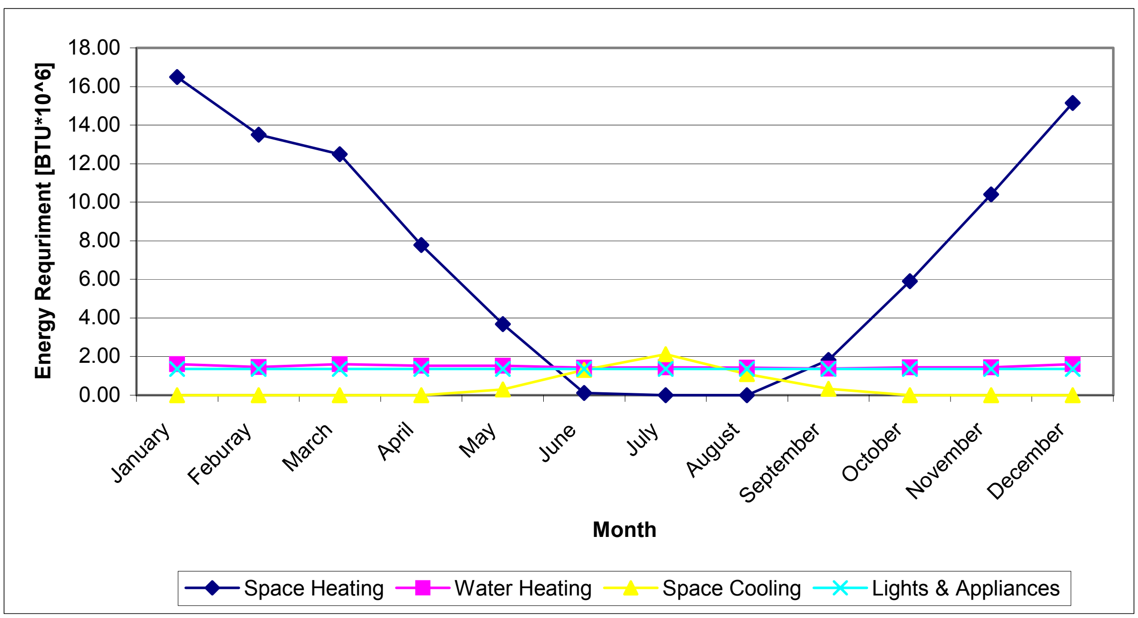

Figure 4.14 Monthly Energy Use, Chicago, Illinois

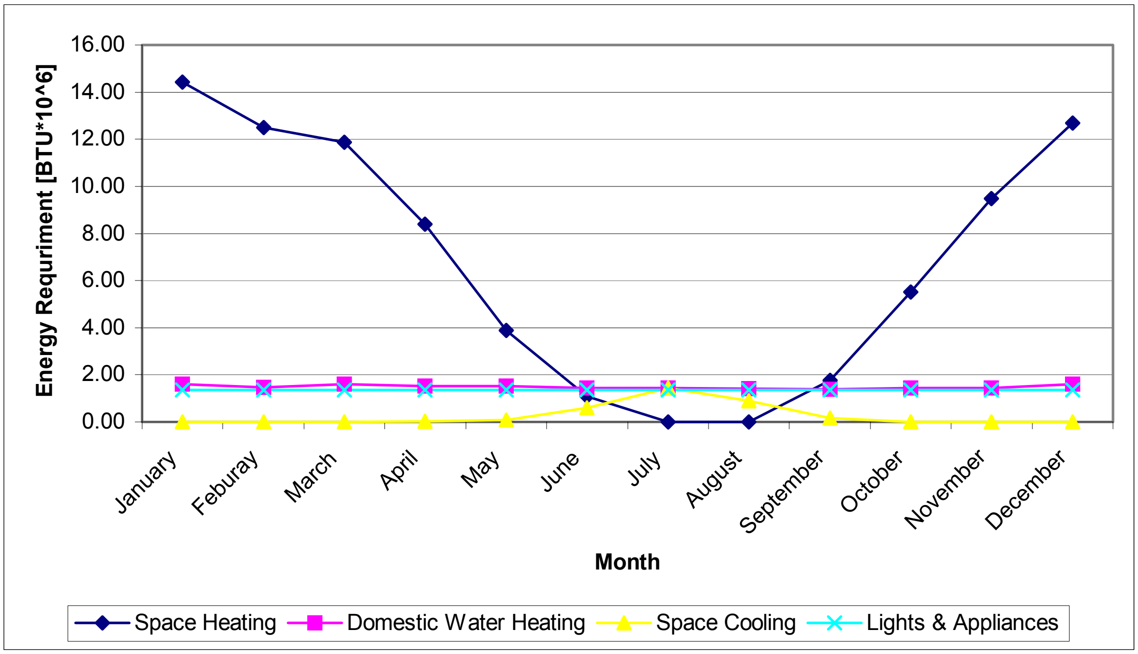

Figure 4.15 Monthly Energy Use Boston, Massachusetts

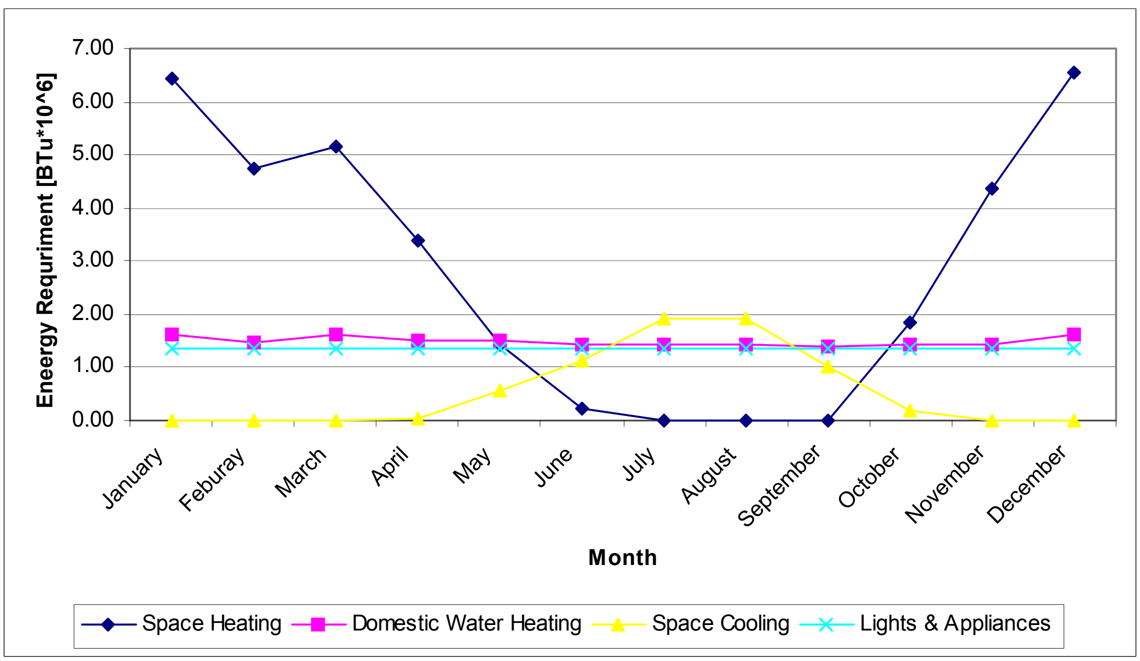

Figure 4.16 Monthly Energy Use Sacramento, California

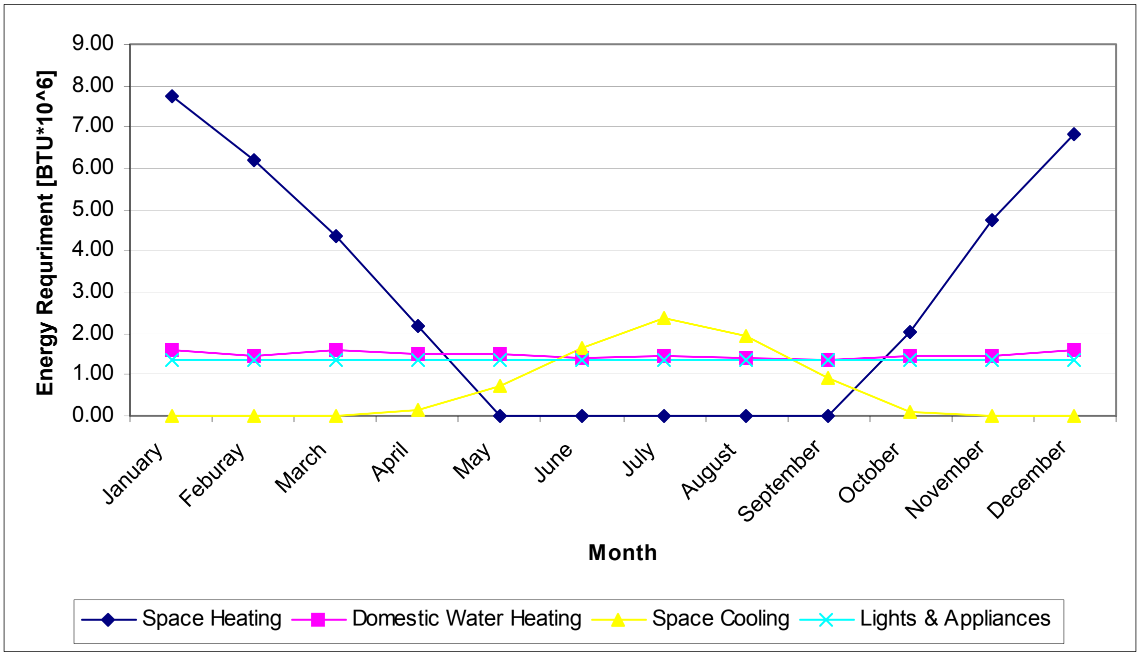

Figure 4.17 Monthly Energy Use Atlanta, Georgia

The energy requirements will also determine the maximum and minimum peak energy use for the various regions. Figures 4.18 through 4.21 provide an hourly profile for a typical summer and winter day in Atlanta, and Boston. The winter loads are much higher than the summer loads with the loads varying from 5.8 kW to 7.89 kW. The average load during the winter for Boston is 6.67 kW, while for Atlanta is 5.87. The summer loads have an average load of 1.5 kW for Atlanta, and 0.82 kW for Boston.

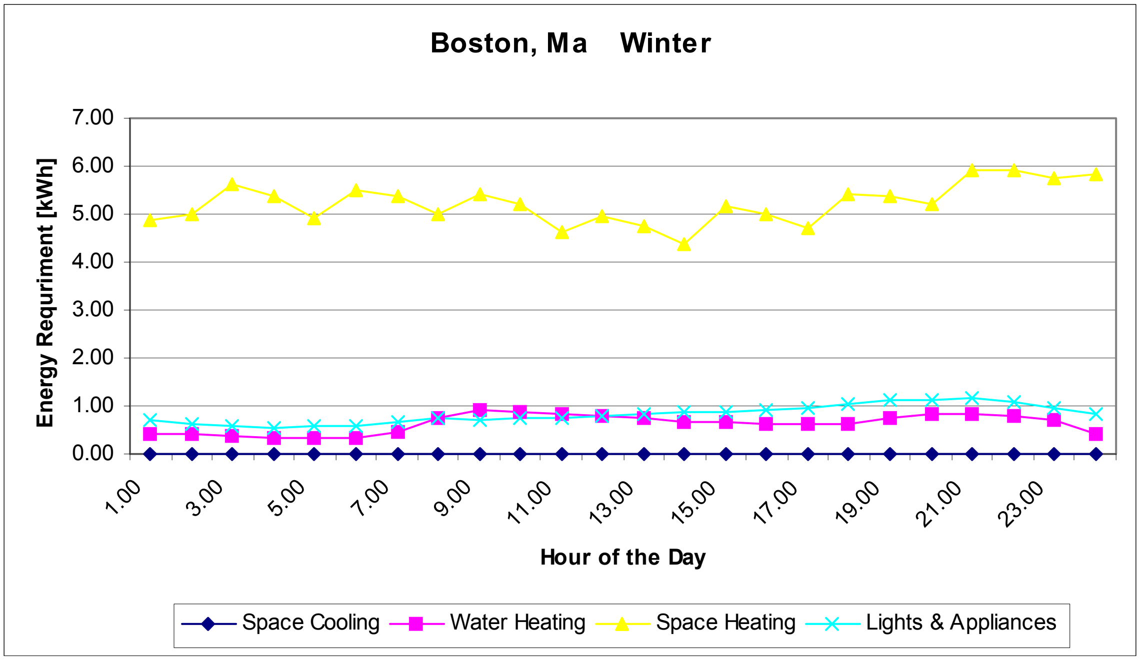

Figure 4.18 Hourly Energy Requirements for Boston, MA (January 15)

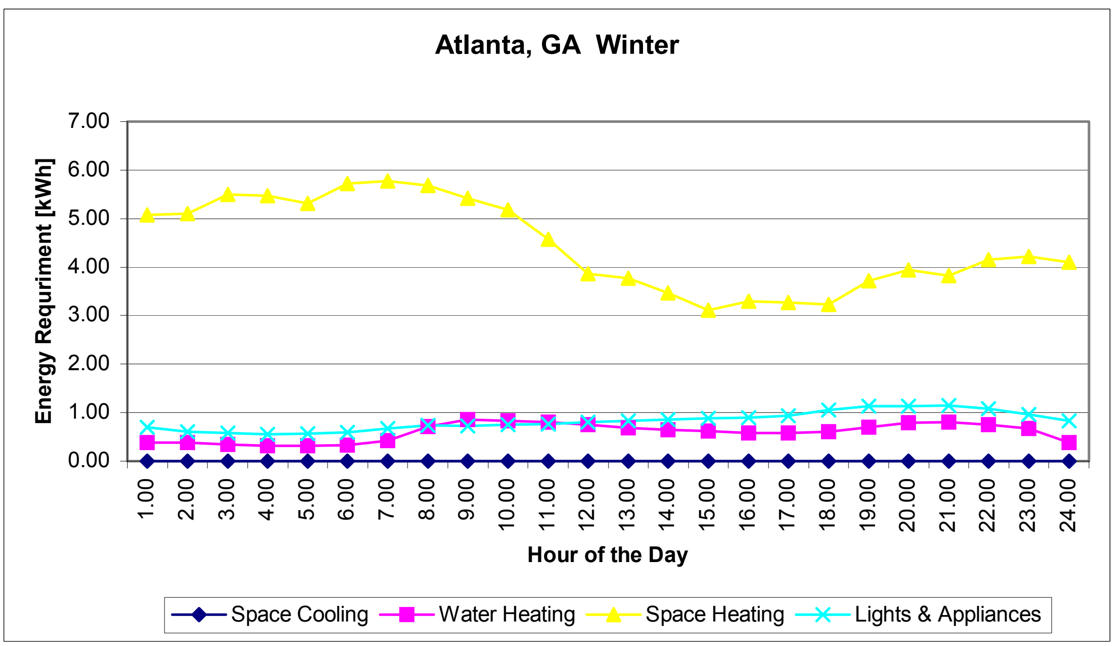

Figure 4.19 Hourly Energy Requirements for Atlanta, GA (January 15)

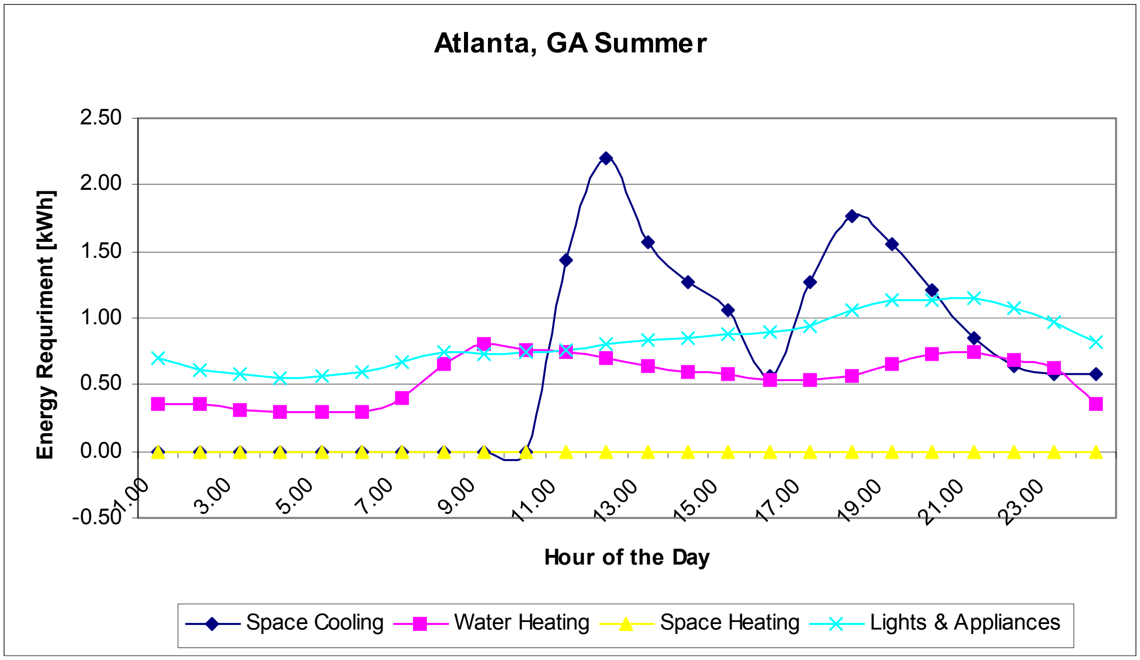

Figure 4.20 Hourly Energy Requirements for Atlanta, GA (July 15)

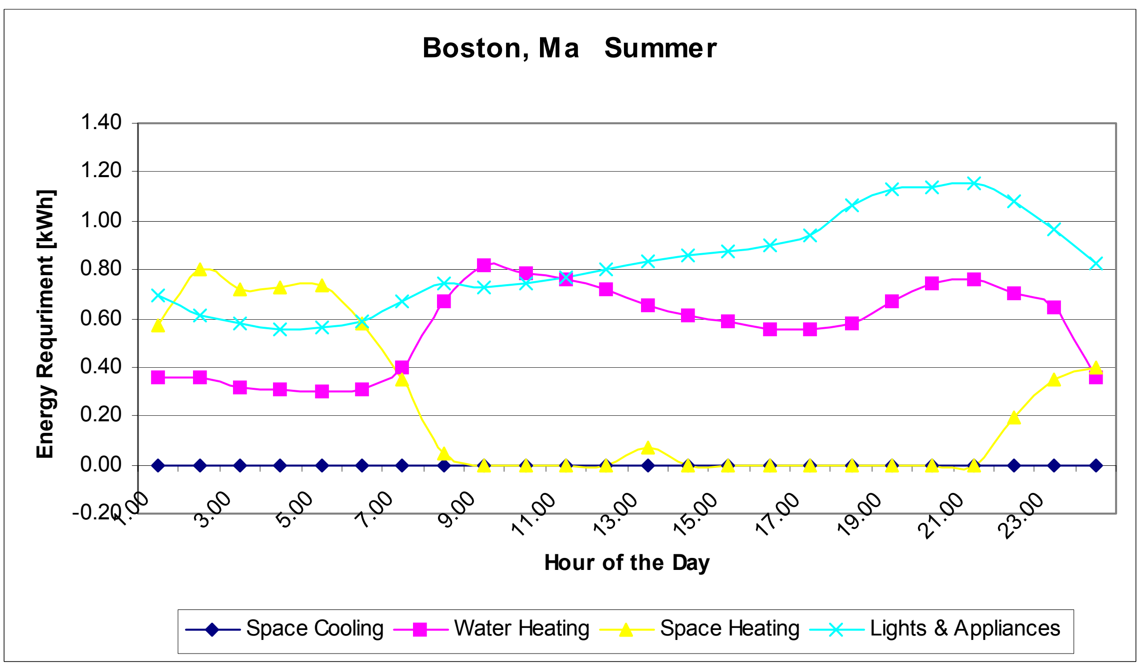

Figure 4.21 Hourly Energy Requirements for Boston, MA (July 15)

4.3.5 Validation of Residential Energy Use

The residential energy characteristics developed in the previous section will be validated by comparing the values with the 1997 Residential Energy Consumption Survey (RECS), conducted by the EIA [1]. The results from the model compare very well with the RECS study. The heating loads are slightly higher in the TRNSYS model, while the cooling loads are slightly lower in the TRNSYS model. Table 4.6 provides the comparison of the yearly space heating and space cooling energy requirements for the TRNSYS model and the RECS survey.

Table 4.6 Comparisons of Yearly Energy Requirements

	Boston		Atlanta	
Yearly	RECS	Model	RECS	Model
Space Heating [MJ/yr]*1000	82	86.11	28.1	35.95
Space Cooling [kWh/yr]	784	939	2665	2187
	Chicago		Sacramento	
	RECS	Model	RECS	Model
Space Heating [MJ/yr]*1000	85.8	92.18	24.4	36.04
Space Cooling [kWh/yr]	1096	1516	1205	1994

4.4 Fuel Cell System

The fuel cell system will be based on a Proton Exchange Membrane (PEM) stack, with a fuel reformer, power conditioner, and thermal recovery system. Figure 4.1 depicts the main components within the fuel cell system. The total efficiency of the system is shown to be the product of the fuel cell stack, system reformer, and the electrical conversion efficiencies.

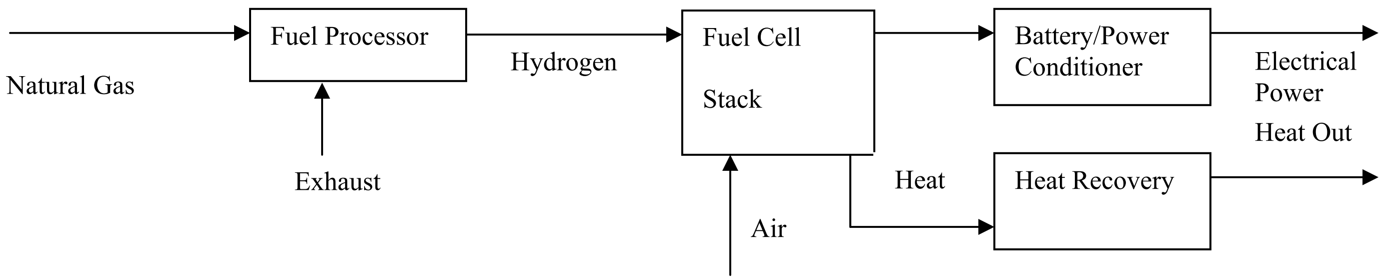

Figure 4.22 Fuel Cell Systems

4.4.1 Fuel Processing

PEMFC operation will require a relatively pure hydrogen fuel to operate. Hydrogen is not readily available, and will need to be generated from a hydrocarbon-based fuel. Natural gas is the most readily available fuel for residential applications, and the ability to extract hydrogen from natural gas may take place by several methods: partial oxidation (POX), autothermal reforming (ATR), or steam reforming (CSR).

Fuel processing will consist of the ability to convert available natural gas to hydrogen available for the fuel cell stack. Fuel processing will encompass the removal of harmful contaminants from the raw fuel, avoiding contamination of the anode stack.

Steam reforming is chosen because of the high conversion efficiency and low concentrations of carbon monoxide. CO concentration needs to be no greater than 10ppm because higher concentrations of CO have the potential to destroy the life of the fuel cell catalysts. Heinzel and Vogel [22]. The steam reforming reactions for natural gas, assuming pure methane are:

$$CH_4 + H_2O \Leftrightarrow CO + 3H_2 \qquad \Delta_R H^0_{298K}(kJ/mol) = 206 \qquad (4.9)$$

$$CH_4 + 2H_2O \Leftrightarrow CO_2 + 4H_2 \qquad \Delta_R H^0_{298K}(kJ/mol) = 165 \qquad (4.10)$$

The overall reaction is highly endothermic, and therefore will require an external heat source, such as a gas-fired burner. The steam reformer developed by Heinzel and Vogel, has been successfully developed and installed (Figure 4.15). The compact steam reformer will include a heat exchanger, a two part-reforming reactor and a radiation burner. The methane and water will pass a heat exchanger where the water is vaporized and heated to the reformer inlet temperature. The first section of the reactor is heated convectively by flue gas, and a low-NOx ceramic radiation burner heats the second section. The product gas passes two fixed bed reactors filled with two catalysts for low and high temperature shift reactions. The experimental study was conducted with a steam-to-carbon ratio of 3-3.5, the ratio of the reformer methane flow to burner methane of 1.35, and atmospheric pressure. The results concluded that the efficiency of the fuel processor after the low temperature shift reaction would be 78.1 %.

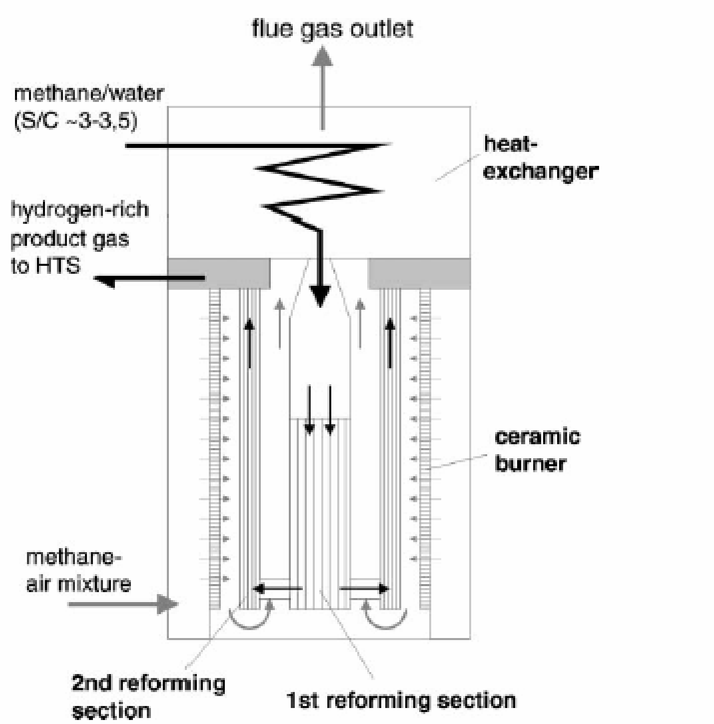

Figure 4.23 Compact Steam Reformers

4.4.1 Fuel Cell Stack

The PEM fuel cell stack will be modeled using the Type170, provided by the HYDROGEMS Inc. [23]. Figures 4.16 and 4.17 graphically represent the construction of the PEM geometry. Figure 4.17 details the geometry of the membrane electrode assembly (MEA) and Figure 4.18 details the geometry of a single fuel cell. The given parameters are listed in the Table 4.6.

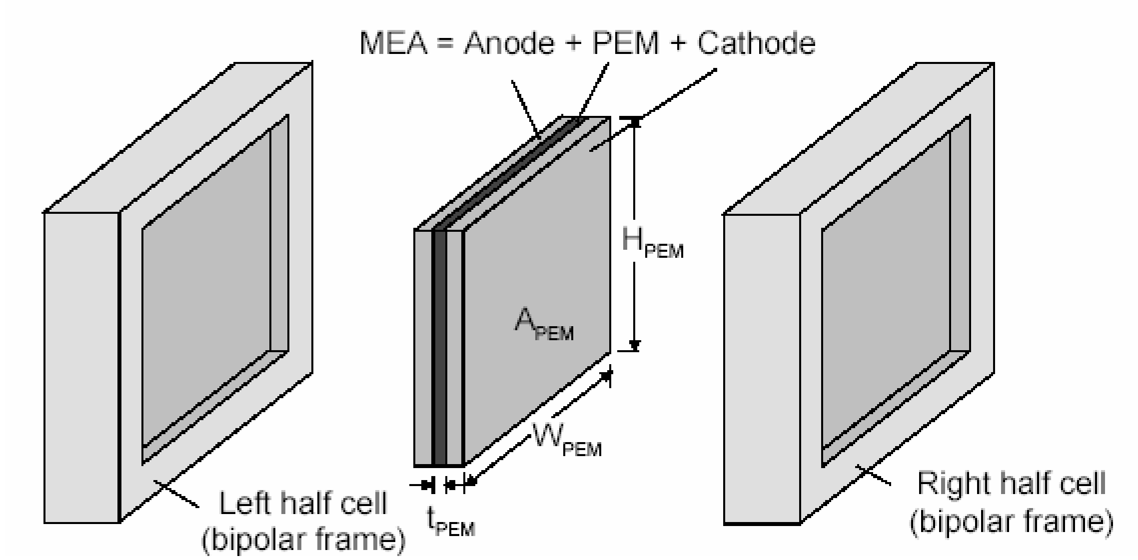

Figure 4.24 Membrane Electrode Assembly

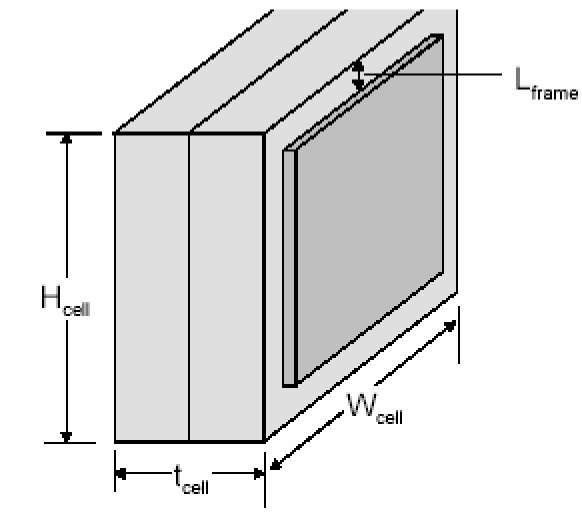

Figure 4.25 Single Fuel Cell

Number	Parameter	Value	Units	Description
1	OXMODE	1		Type of Oxidant feed to cathode
				OXMODE=1: Air
				OXMODE=2: Oxygen
2	TMODE	1		Temperature Mode
				TMODE=1 Static Model (T_{fc} given)
				TMODE=2 Static Dynamic Model
3	η_{cells}			Number of Cells in Series per Stack
4	η_{stacks}			Number of Stacks in Parallel per unit
5	A_{PEM}		cm^2	Electrode Area (cross-sectional) of PEM
6	t_{PEM}		cm	Thickness of PEM
7	γ			Transport Number for water
				0.0= well hydrated
				1.2= Water deficient
8	$U_{c, min}$		V	Minimum allowable cell voltage
9	i_{max}		mA/cm^2	Maximum Allowable current density
10	$RTCT_{Mode}$			Modes for calculating thermal coefficients
RTCTMODE =1				
11	h_{air}		$W/m^2{*}K$	Heat Transfer Coefficient to ambient air
				5-50 for Natural Convection
				50-250 for forced convection
12	Acell		cm^2	Cross Sectional Area of Cell
13	t_{cell}		cm	Thickness of Cell

Table 4.7 Type170 Parameters

Chapter 3.3 described the losses due to activation losses, pressure and gas concentrations, and ohmic losses; therefore the fuel cell stack will not operate at maximum efficiency. The pressure and gas concentration will modeled by the Nernst equation:

$$E = 1.229 + \frac{RT}{2F} Ln\left[\frac{p_{H2O} \cdot p_{O2}^{1/2}}{p_{H2O}}\right] \tag{4.11}$$

The activation losses will be broken into the anode and cathode overvoltages. The anode overvoltage is described by equation 4.12

$$\eta_{act,a} = -\frac{\Delta G_{ec}}{2F} + \frac{RT}{2F} Ln\left(4FAk_a^o c_{h2}^*\right) - \frac{RT}{2F} Ln(i) \tag{4.12}$$

The cathode overvoltage may be expressed by equation 4.13

$$\eta_{act,c} = \frac{RT}{\alpha_c Fn}\left(Ln\left[nFAk_c^o \exp\left(-\frac{\Delta G_{ec}}{RT} \right) * \left(p_{o2}^*\right)^{(1-\alpha)} \left(p_{H2}^*\right)^{(1-\alpha)} \left(p_{h20}^*\right)^{\alpha} \right] - Ln(i) \right) \qquad (4.13)$$

Where ΔG_{ec} and k_a^o and α are chemical parameters of the reaction, and explained in detail by Berger [24].

An empirical relation derived by equation 4.14 will analyze the ohmic voltage, r_m,

$$r_m = \frac{181.6\left[1 + 0.03\left(\frac{i}{A}\right) + 0.062\left(\frac{T}{303}\right)^2 \left(\frac{i}{A}\right)^{2.5}\right]}{\left[\lambda - 0.634 - 3\left(\frac{i}{A}\right)\right] \exp\left(4.18\left[\frac{T-303}{T}\right]\right)} \qquad (4.14)$$

The parameter λ represents an empirical correction of the effect of the average water content of the membrane-current density and cell temperature. The value of λ will have the value of 1 for a well hydrated and a value of 0 for a dry cell. The cell voltage with the appropriate loss calculations decreases with increasing current density at stoichiometric and constant pressure conditions. (Figure 4.26)

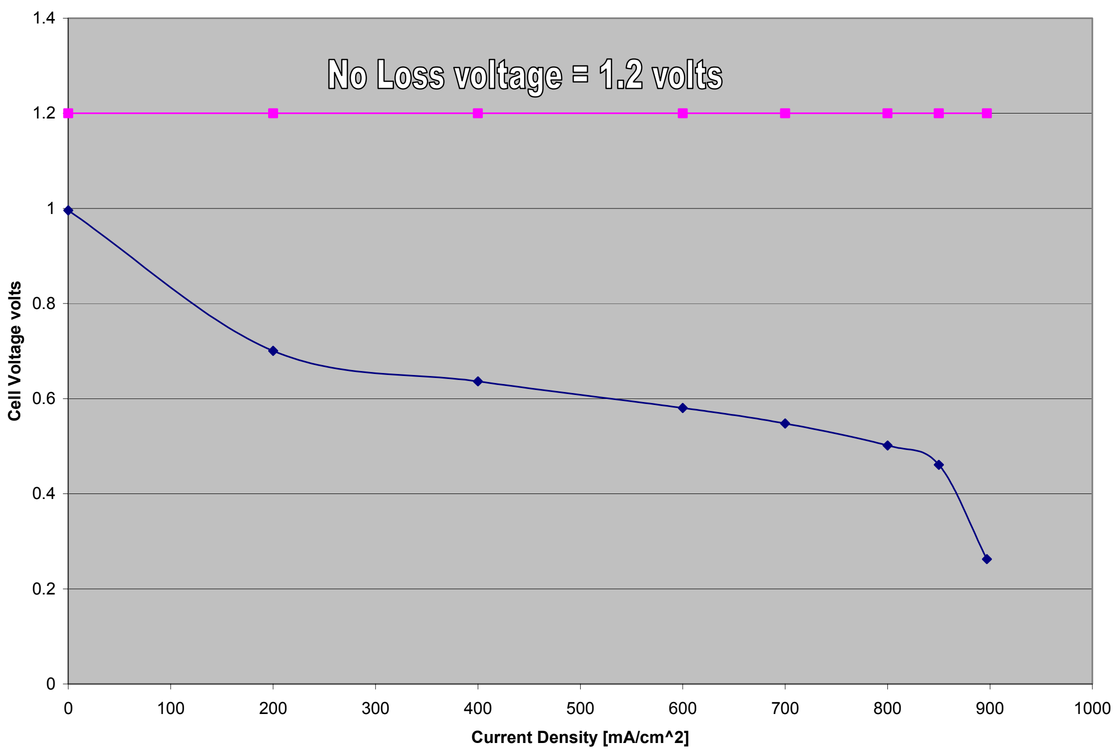

Figure 4.26 Cell Voltage vs. Current Density

4.4.1.1 Faraday Efficiency

Faraday's Law (4.15) will determine the stoichiometric amount of hydrogen, supplied to the fuel cell.

$$n_{H_2} = \frac{n_c I}{nF} \tag{4.15}$$

The performance of the fuel cell will be determined by the flow rates of hydrogen and oxygen to either side of the stack, in general the molar amount of oxygen supplied to the cathode will be twice the molar amount of hydrogen.

An increase in the amount of oxygen supplied will increase the stack performance (Figure 4.27).

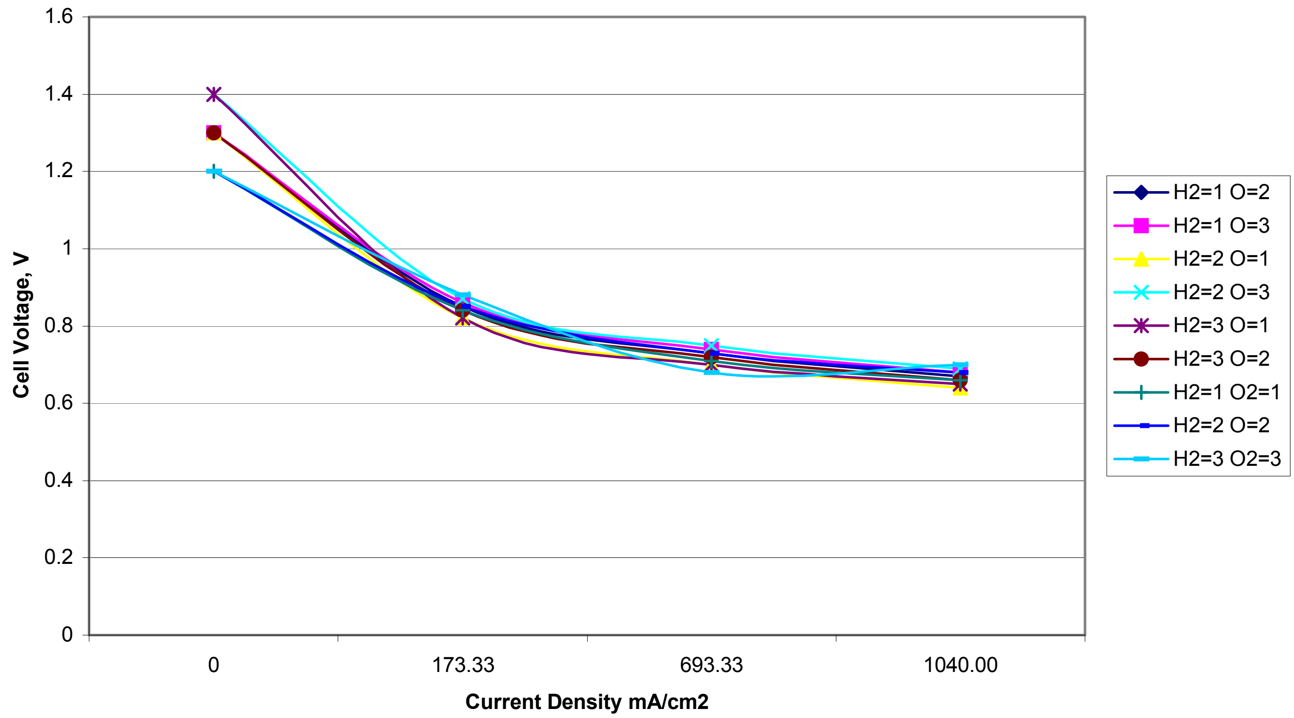

Figure 4.27 Stoichiometric effects of Hydrogen and Oxygen on Cell Voltage

4.4.1.2 Fuel utilization

Fuel Utilization is the concept that not all of the fuel inputted to the fuel cell is actually used. The efficiency of fuel utilization is the mass of the fuel reacted in the cell divided by the mass of the fuel input to the cell (4.16).

$$n_f = \frac{n_{H_2 Stoic}}{n_{H_2 actual}} \tag{4.16}$$

4.4.2.3 Pressure

The operating pressure at the inlet of the fuel cell will consist of the hydrogen determined by the reformer outlet pressure, which will be assumed at 1 bar. The air inlet pressure remains at atmospheric conditions. Increasing the air pressure will increase the efficiency of the fuel cell and the penalty may be seen in Figure 4.28

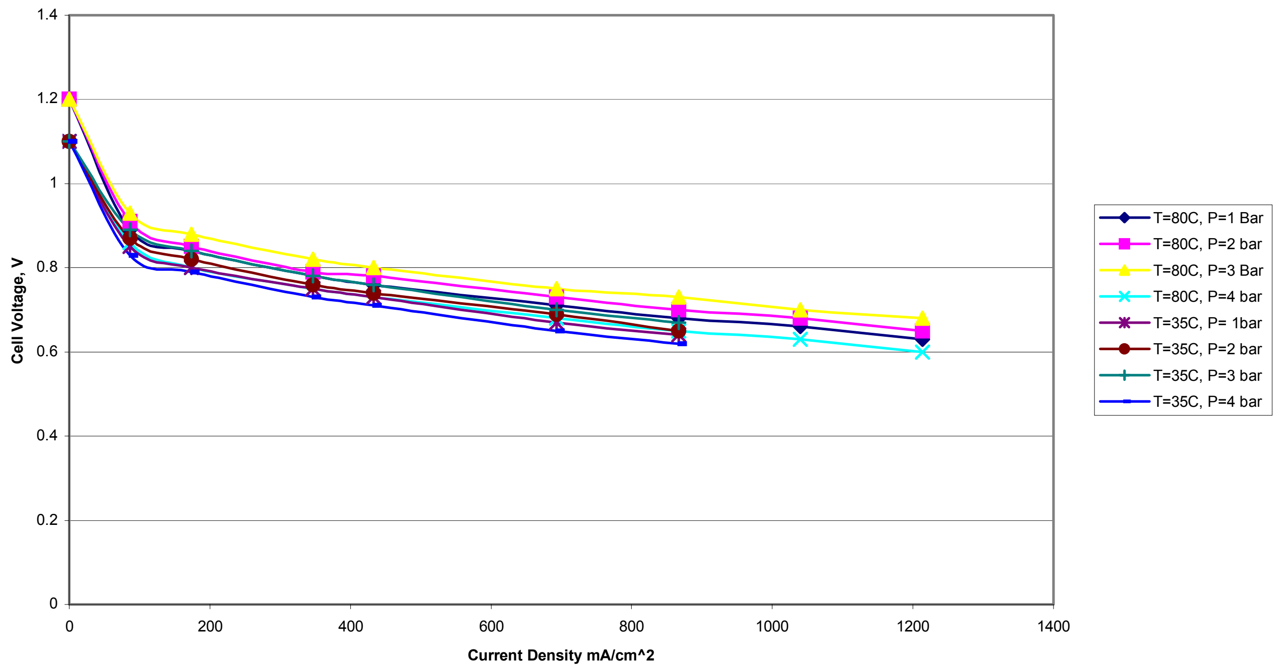

Figure 4.28 Effect of Inlet Air Pressure on Cell Voltage

4.4.2.4 Thermal Model

Mass and Energy balances around the fuel cell stack where developed to determine various energy terms associated with the fuel cell operation, which include the internal heat generation, thermal energy storage, the heat loss from to the environment, and auxiliary cooling. [25]

$$\dot{q}_{gen} = \dot{q}_{store} + \dot{q}_{Loss} + \dot{q}_{cool} \quad (4.17)$$

$$q_{gen} = n_c(V - V_{tn})I = n_c VI(1 - n_e) \quad (4.18)$$

$$q_{store} = C_t \frac{dT}{dt} \quad (4.19)$$

$$q_{loss} = \frac{1}{R_t}(T - T_a) \quad (4.20)$$

$$q_{cool} = C_{cw}\left(T_{cw,i} - T_{cw,o}\right) \quad (4.21)$$

Equation 4.21 is the required amount of cooling needed for the fuel cell to stay at its operating temperature, and the fuel cell will utilize cooling cells between the stacks to for proper cooling. The cooling cells will operate with water, to increase the thermal conductivity, and each cell will be placed between every 5 fuel cells. The cooling cells will act as a heat exchanger and will be discussed in chapter 4.6 the transient prediction of the fuel cell stack may be predicted by the following:

$$MC\left(\frac{dT_{stack}}{dt} = \dot{q}_{theo} - \dot{q}_{elec} - \dot{q}_{sens} - \dot{q}_{loss}\right) \quad (4.24)$$

4.4.2.5 Fuel Cell Stack Validation

The transient information needed to model a fuel cell in TRNSYS is detailed and the evaluation of the fuel cell stacks it self has been modeled against experimental data on a Ballard 5kW system [26]. The stack consisted of 35 cells with an electrode area 230cm^2.

Figure 4.22 shows the parametric model with the given parameters and the total output voltage. The graph verifies that the TYPE170 component agrees very well with the experimental data taken on the Ballard fuel cell stack.

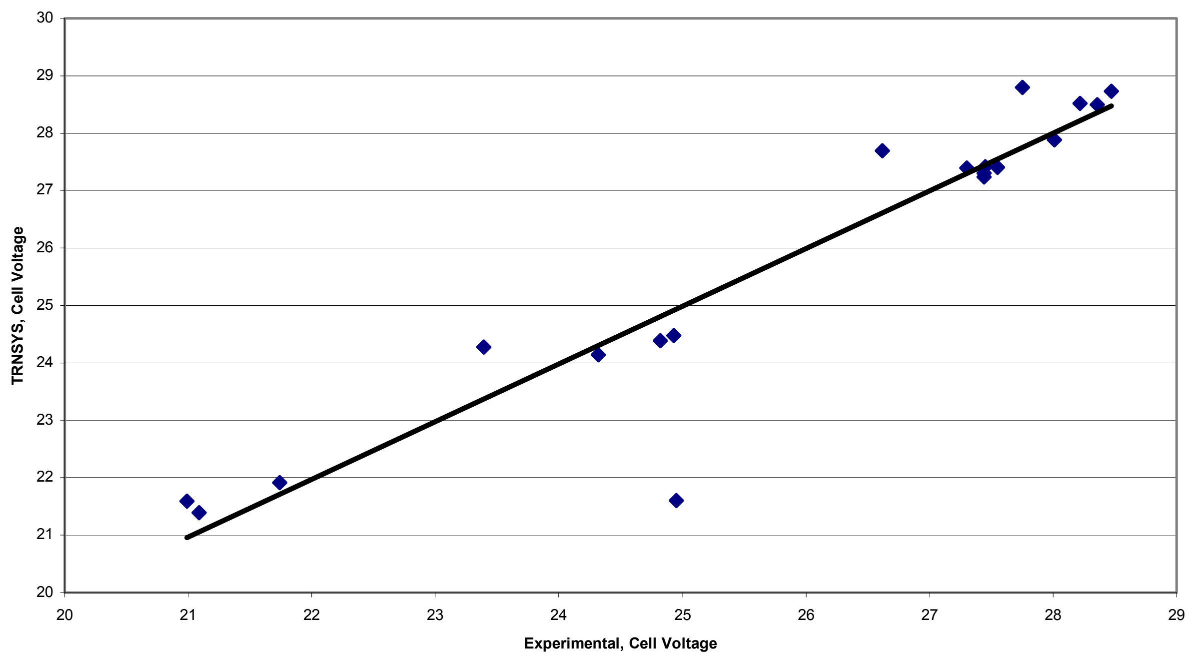

Figure 4.29 Comparison of Experimental and Model Cell Voltage

4.4.2.6 Power Conditioning

The power-conditioning unit is designed to convert the DC power into AC power at the appropriate voltage available for residential applications. The power loss for the power conditioner is dependent on the current running through it Laukamp [27] suggested a three-parameter relationship for the power loss:

$$P_{Loss} = P_{in} - P_{out} = P_o + \frac{U_s}{U_{out}} P_{out} + \frac{R_i}{U_{out}^2} P_{out}^2 \qquad (4.25)$$

A relationship between the power input and the power output is determined by normalizing equation 4.25 with respect to the maximum power output:

$$\frac{P_{in}}{P_{nom}} = \frac{P_o}{P_{nom}} + \left(1 + \frac{U_s}{U_{out}}\right)\frac{P_{out}}{P_{nom}} + R_i P_{nom}\left(\frac{P_{out}}{P_{nom}}\right)^2 \quad (4.26)$$

The efficiency of the power conditioner may now be determined as:

$$\eta = \frac{P_{out}}{P_{in}} \quad (4.27)$$

4.5 Thermal Storage Tank

The thermal storage tank will be modeled by using a Type60 stratified fluid storage tank using a multi node approach. The multi node approach involves dividing the tank into N segments or nodes and performing an energy balance for each node. The tank will consist of N equal nodes, if one node is selected the tank will assume a fully mixed tank, and increasing the number of nodes will decrease internal mixing and a higher degree of thermal stratification is achieved. It is necessary to determine the minimum number of nodes to find an accurate amount of degree of stratification, the tank may have a maximum number of 100 nodes, but increasing the number of nodes greatly increases the computing time. The simulation was run for one month, with a constant to determine the number of nodes necessary for the simulation, Figure 4.30 shows the effect of the percentage of heat provided for various flow rates.

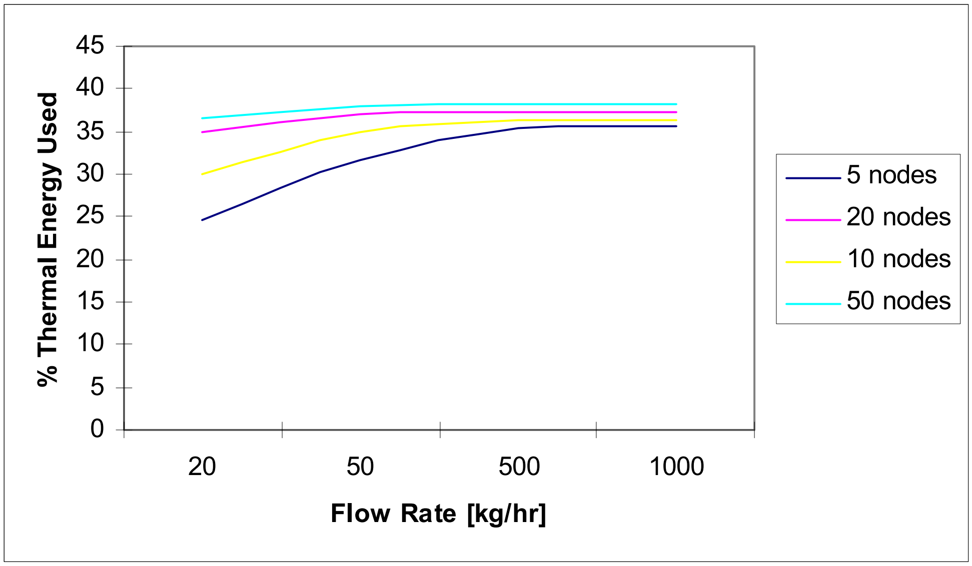

Figure 4.30 Effect of Number of Nodes per Cell Area

Increasing the number of nodes increases the degree of stratification and therefore increases the amount of heat provided from the fuel cell system. It can be seen that the difference between 50 and 20 nodes is negligible; therefore 20 nodes shall be used for all simulations. The optimal flow may also be found from analyzing Figure 4.30, it can be seen that the fraction of heat provided stay consist with increasing higher flow rates. The optimal flow through the fuel cell system loop shall be 1000 kg/hr.

The storage tanks will be assumed to be located within a garage or a crawlspace and the environmental temperature is defined by equation 4.28

$$T_{env}=T_{amb} + (22- T_{amb})/3 \qquad (4.28)$$

4.6 Heat Exchanger

The process of heat exchange between two fluids that are at different temperatures and separated by a solid wall is known as a heat exchanger. Heat exchangers are classified according to flow arrangement and type of construction. A concentric tube heat exchanger transfers heat for which the hot and cold fluids move in the same or opposite directions. Parallel-flow heat exchangers, the fluids enter at the same section, flows in the same direction, and exit at the same end. Counterflow heat exchanger, the fluid enters at opposite ends, flow in opposite directions, and leave at opposite ends. Shell-and-tube heat exchangers are dependent on the number of shell-and-tube passes, but the simplest form involves a single tube and shell passes.

The effectiveness of a heat exchanger is defined as the ratio of the actual heat transfer to the maximum possible heat transfer. The fuel cell system will operate with cooling cells flowing in-between the cell stacks. The construction of the cell stack with the cells running through them may be modeled as a cross-flow heat exchanger. The heat generated within the stack will be transferred to the water flowing within the tubes. The temperature of the heat generated will stay at a constant 70°C. [28]. The constant temperature will allow for the average temperature difference to be determined by the log mean temperature difference.

$$\Delta T_{lm} = \frac{(T - T_{cw,i}) - (T - T_{cw,o})}{LN[(T - T_{cw,i})/(T - T_{cw,o})]} \tag{4.29}$$

The temperature of the water at the outlet of the tube is determined by equation 4.30:

$$T_{cw,o} = T_{cw,i} + (T - T_{cw,i})\left[1 - \exp\left(\frac{UA_{HX}}{mc_p}\right)\right] \tag{4.30}$$

Where the UA_{HX} is the overall heat transfer coefficient of the heat exchanger, and will be the dimensioning parameter for the heat exchanger analysis.

The effectiveness of a cross flow heat exchanger with one fluid mixed is defined in equation 4.31, while the outlet temperature is described in equation 4.32.

$$\varepsilon_1 = 2\left\{1+\frac{C_{\min}}{C_{\max}}+\left(1+\left(\frac{C_{\min}}{C_{\max}}\right)^2\right)^{0.5} * \frac{1+\exp\left[-\frac{UA}{C_{\min}}\left(1+\left(\frac{C_{\min}}{C_{\max}}\right)^2\right)^{0.5}\right]}{1-\exp\left[-\frac{UA}{C_{\min}}\left(1+\left(\frac{C_{\min}}{C_{\max}}\right)^2\right)^{0.5}\right]}\right\}^{-1} \tag{4.31}$$

$$T_{ho} = T_{hi} - \varepsilon\left(\frac{C_{\min}}{C_h}\right)\left(T_{hi} - T_{ci}\right) \tag{4.32}$$

The number of transfer units, NTU, is a dimensionless parameter that indicates the heat exchanger size and is represented by equation 4.33:

$$NTU=UA/Cmin \tag{4.33}$$

The NTU relation will allow for the design of an optimal heat exchanger size based on varying flow rates of either side of the heat exchanger.

4.7 Economics

The economics of the CHP system will be evaluated by determining the life cycle costs of the system, and compare them to the life cycle costs of a conventional system. The determination of the life cycle costs will be based on the cost of electricity for each system.

4.7.1 Cost of Electricity

The fuel cell system will be evaluated by determining the cost of electricity that has been researched by Barbier and Gomez [29]; they determined that the cost of electricity is for a fuel cell system will consist of the capital cost, fuel cost, and operation and maintenance. The annualized the three factors and found that the cost of electricity may be determined by equation 4.7.1:

$$C_{el} = \frac{\left[\left(C_{fc} * \left(\frac{d(1+d)^L}{(1+d)^L - 1}\right)\right) + \left(C_f * \frac{P_{fc} * 8760 * \frac{CF}{1000}}{\eta}\right)\right]}{P_{fc} * 8760 * \frac{CF}{1000}} \tag{4.7.1}$$

Where:

C_{fc} = Fuel cell stack cost ($)

C_f = Cost of fuel ($/kWh)

P_{fc} = Nominal power output [W]

CF = Capacity factor

d = Interest rate

L = Lifetime (yrs)

From equation 4.7.1 it can be shown that the dimensioning parameter will be the fuel cell stack cost, which to this date is approximated as $294/cell [30], which includes the cost of a fuel processor, and balance of plant operations. The capacity factor is defined as the annual part load ratio of the fuel cell system. The cost of fuel will be determined from information provide by EIA Annual Energy Outlook, which may be found on the EIA website. The cost of natural gas for the four locations of interest is presented in Table 4.7.1.

Table 4.7.1 Projected Energy Prices										
Electricity (c/kWh)	**2003**	**2004**	**2005**	**2006**	**2007**	**2008**	**2009**	**2010**	**2011**	**2012**
Boston	10.41	10.27	10.05	9.83	9.77	9.90	9.81	10.16	10.25	10.54
Chicago	7.27	7.19	7.10	6.99	6.80	6.80	6.69	6.79	6.80	6.91
Atlanta	7.65	7.71	7.71	7.56	7.43	7.39	7.39	7.47	7.51	7.52
Sacramento	8.93	8.69	8.68	8.64	8.75	8.86	8.96	9.04	9.00	8.84
Natural Gas ($/MMBtu)	**2003**	**2004**	**2005**	**2006**	**2007**	**2008**	**2009**	**2010**	**2011**	**2012**
Boston	9.95	9.71	9.55	9.46	9.44	9.48	9.55	9.63	9.71	9.78
Chicago	6.70	6.50	6.40	6.30	6.33	6.38	6.45	6.55	6.62	6.68
Atlanta	8.79	8.45	8.30	8.17	8.18	8.21	8.27	8.39	8.45	8.51
Sacramento	7.20	7.25	7.35	7.34	7.33	7.51	7.56	7.60	7.58	7.56
Electricity (c/kWh)	**2013**	**2014**	**2015**	**2016**	**2017**	**2018**	**2019**	**2020**	**2021**	**2022**
Boston	10.65	10.82	10.84	10.98	11.03	11.15	11.24	11.34	11.31	11.28
Chicago	6.91	6.98	6.91	7.02	6.92	7.00	6.91	7.06	6.95	7.07
Atlanta	7.55	7.57	7.57	7.57	7.57	7.58	7.59	7.60	7.61	7.63
Sacramento	8.83	8.88	8.93	8.99	9.00	8.99	8.97	8.98	9.01	9.07
Natural Gas ($/MMBtu)	**2013**	**2014**	**2015**	**2016**	**2017**	**2018**	**2019**	**2020**	**2021**	**2022**
Boston	9.83	9.85	9.85	9.89	9.81	9.79	9.79	9.81	9.74	9.72
Chicago	6.74	6.78	6.81	6.84	6.84	6.80	6.81	6.90	6.88	6.92
Atlanta	8.55	8.53	8.51	8.53	8.54	8.47	8.48	8.60	8.63	8.66
Sacramento	7.47	7.60	7.67	7.70	7.66	7.65	7.61	7.64	7.51	7.62

Table 4.7.1 Projected Energy Prices

The evaluation of the cost of electricity will also include the maintenance costs, and for a fuel cell system the only major maintenance cost will consist of replacing the fuel cell stack every 5 years, which will span the lifetime analysis [31]. The interest rate is 10% for the fuel cell system.

4.7.1 Life Cycle Analysis

The concept of life cycle costing includes both the initial capital cost and the year-to-year operating cost. The life cycle cost is the total of the; capital equipment cost, acquisition costs, operating costs, interest charges, maintenance, taxes, and the salvage value.

The life cycle cost may be determined by equation 4.34:

$$LCC = IC + \sum_{i}^{l} \frac{AEU * C_f}{(1+d)^i} + \sum_{i}^{l} \frac{MC}{(1+d)^i} \qquad (4.7.2)$$

Where;

IC = Initial Cost of the System ($)

AEU = Annual Energy Use (kWh)

MC = Maintenance Cost ($)

The initial cost of the system can be determined by evaluating the equipment prices available in Table 4.7.2.

Table 4.7.2		
All Electric System		**Dollars**
Complete HVAC System		2900
Electric Water Heater		720
Maintenance		400
Total		**4,020**
Natural Gas/Electric System		
AC System (SEER=10)		800
Furnace		850
Gas Water Heater		1100
Maintenance		400
Installation		1200
Total		**4,350**
Combined Heat and Power System		
Fuel Cell System		13000
Thermal Storage Tank	40 Gallon	320
	80 Gallon	1090
Thermal Space Heating Coil		600
Total		**21,010**

The equipment prices for each system have been determined form Grainger [28] engineering equipment catalog. Table 4.7.1 provides the cost of electricity and natural gas for the respective locations of this research. The maintenance cost for the fuel cell system have will be neglected in the determination of the life cycle analysis because the maintenance costs have been factored into the cost of electricity for the fuel cell system.

Chapter 5 Results

This section will describe the design considerations and energy use characteristics of the combined heat and power fuel cell system. The required fuel cell system size, minimum heat exchanger size, and thermal storage tank size are analyzed.

5.1 Conventional Systems

Two conventional systems shall be analyzed, as a comparison to the CHP system. The first system is an all-electric system. It will consist of an electric vapor heat pump (SEER=10), and electric resistance water heating. An electric AC unit will provide the space cooling. The second system will consist of natural gas furnace for space heating and a natural gas water tank for domestic water heating. There will be an electric air-conditioner for space cooling as well.

5.1.1 All Electric System

This system will use electricity for space heating, cooling and water heating. A separate TRNSYS model was developed top determine the energy requirements for this system. The model consisted of an electric resistance water tank, which assumes all of the electric input will be converted into usable heat for the water. An electric heat pump is used to fulfill the space heating and cooling loads. The results are summarized in table 5.1:

End-Use (kWhe)	**Boston**	**Chicago**	**Atlanta**	**Sacramento**
Lights & Appliances	4800	4800	4800	4800
Space Cooling	932	1422	1267	1868
Space Heating	10278	10200	4451	3877
Water Heating	5196	4980	4962	4962
Storage Tank Heat Loss	685	698	649	659
Total Electricity	***21891***	***22100***	***16129***	***16166***

Table 5.1 Annual Electric Usage-All Electric System

The results indicate the expected, that the colder climates have a higher electricity usage than the warmer climates and this is due in part to the high space heating loads.

5.1.2 Electric & Natural Gas System

Natural gas is another common source of energy for residential applications, and this section will look at a system that consists of natural gas for space heating and water heating. The space cooling loads will be meet by an electric air conditioner. The natural gas furnace will have an efficiency of 0.7, while the natural gas hot water tank will have an efficiency of 0.85. The results are presented in Table 5.2

	Boston	**Chicago**	**Atlanta**	**Sacramento**
End-Use (Kwhe)				
Lights & Appliances	4800	4800	4800	4800
Space Cooling	932	1422	1267	1868
Total Electricity	**5732**	**6222**	**6067**	**6668**
Space Heating (kWh)	34260	34000	14837	12922
Water Heating (kWh)	932	1422	1267	1868
Space Heating (n=0.7)	44538	44200	19288.1	16798.6
Water Heating (n=0.85)	1071.8	1635.3	1457.05	2148.2
Total Natural Gas (MJ)	***164195***	***165007***	***74683***	***68208***

Table 5.2 Annual Electric and Natural Gas System

The results are exactly the same as the all-electric system; in the total energy use varies from the cold climates, to the warmer climates.

5.2 Combined Heat & Power System

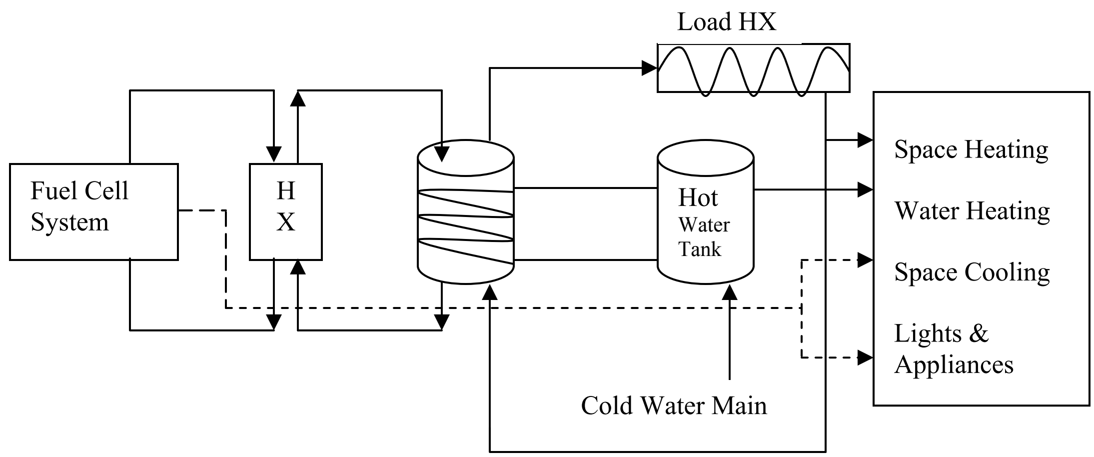

Figure 5.1 Schematic of the Combined Heat and Power System

The CHP system analyzed in this research can be seen again in Figure 5.1

5.2.1 Fuel Cell System

The amount of electricity provided to the residence from the fuel cell system must be an adequate amount to meet the maximum average hourly demand as predicted in the model. This research looked at the maximum power demand for lights, appliances, and space cooling. The power conditioning equipment will provide any peak power demands associated with motor starts, and any miscellaneous power surges. Table 5.3 provides the maximum peak power demands for each city.

Table 5.3 Averaged Peak Power Demands (kW)		
	Space-Heating	Non-Space Heating
Boston	6.67	0.82
Chicago	6.71	1.22
Atlanta	5.87	1.5
Sacramento	5.42	1.43

Table 5.3 details that sizing a fuel cell system to meet the space heating demand will require a very large system. Increasing the fuel cell system will increase the amount of heat available for space heating, but will reduce the overall cogeneration efficiency because the large amount of usable heat will be wasted during the summer months when space heating is not required. Increasing the fuel cell system will also increase the cost of the system, which will drastically increase the life cycle savings of the system. The designed fuel cell system for all locations will consist of a 1.5 kW fuel cell stack, which will consist of 24 cells with an electrode area of 245 cm^2. Figures 4.27 detail the affect of the stoichiometric amount of hydrogen and oxygen on the PEM fuel cell stack, and the system will run at stoichiometric rates of 2.5 and 1.5 for air and hydrogen respectively. Figure 4.28 details the effects of varying the inlet air pressure, and for this system the air pressure will be at a constant 1 bar. The hydrogen inlet pressure will also run at 1 bar.

5.2.2 Heat Exchanger

In order to determine the optimal flow rate for the heat exchanger TRNSYS various simulations where run with varying flow rates for the hot side of the heat exchanger, ranging from 250-1500 kg/hr. The simulation was run with a storage tank capacity of 80-gallons, and a hot water storage tank size of 40 gallons. The amount of rejected heat from the fuel cell system that may be utilized for thermal applications will be defined as the percentage of usable heat, and it has been calculated for various values of a modified NTU value. The modified NTU value is defined as the overall heat transfer coefficient over the capacitance rate of the fuel cell side of the heat exchanger, $UA/mc_{p,FC}$, regardless whether $mc_{p,FC}$ was the minimum capacitance rate in the collector-storage tank heat exchanger. The simulations where run with different ratios of the hot side of the collector over the storage tank side of the collector, ranging from 0.5-3.0.

Figures 5.2-5.5 represent the percent of usable heat as a function of NTU for various ratios of $mc_{p,FC}$ and $mc_{p,tank}$. Each Figure represents a different constant fuel side flow rate.

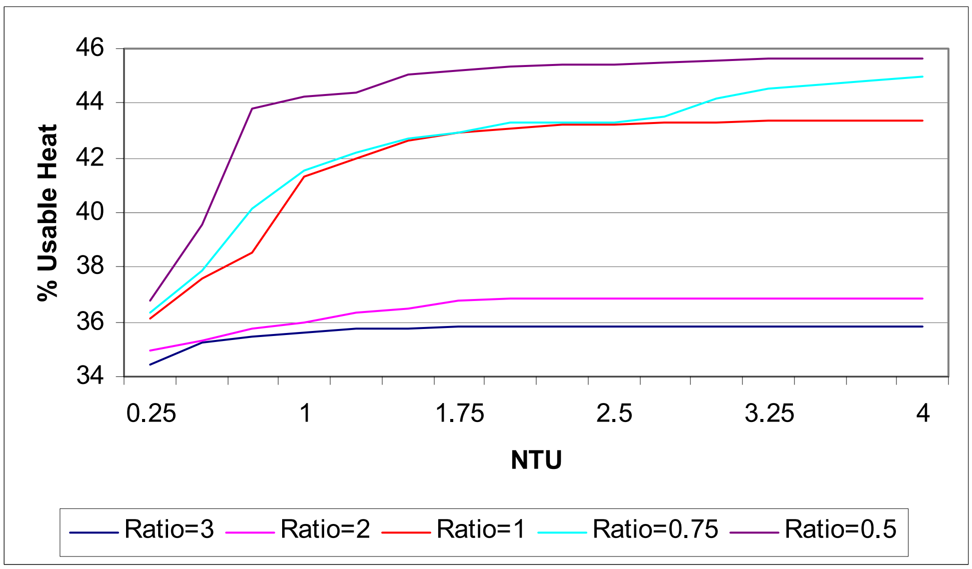

Figure 5.2 NTU vs. Percent Usable Heat for Hot Side Flow Rate of 250 kg/hr

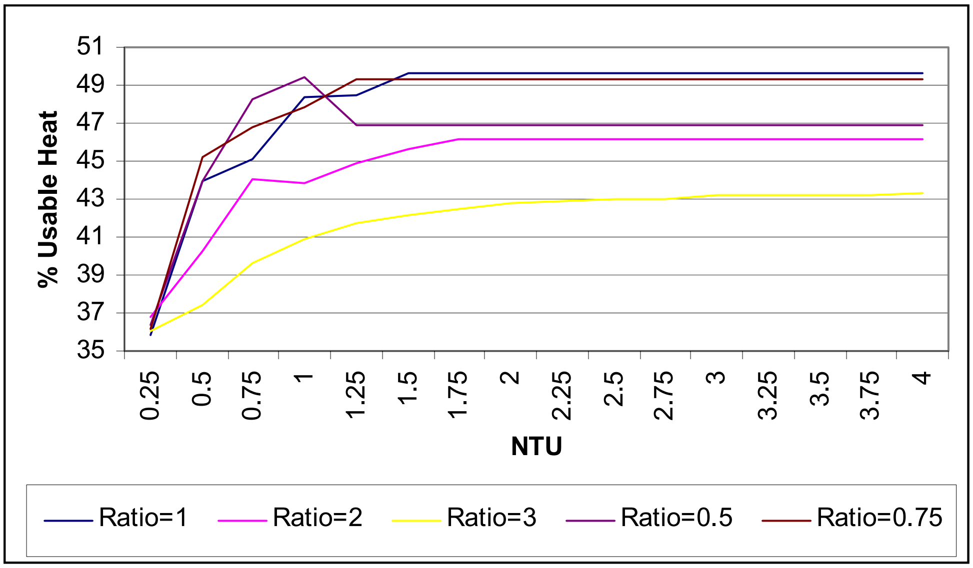

Figure 5.3 NTU vs. % Usable Heat for Hot Side Flow Rate of 500 kg/hr

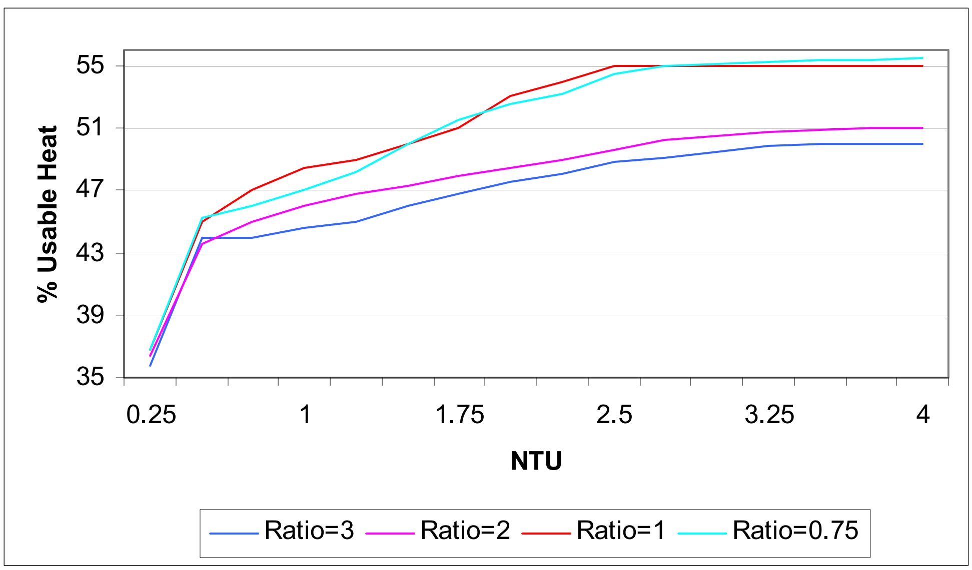

Figure 5.4 NTU vs. % Usable Heat for Hot Side Flow Rate of 1000 kg/hr

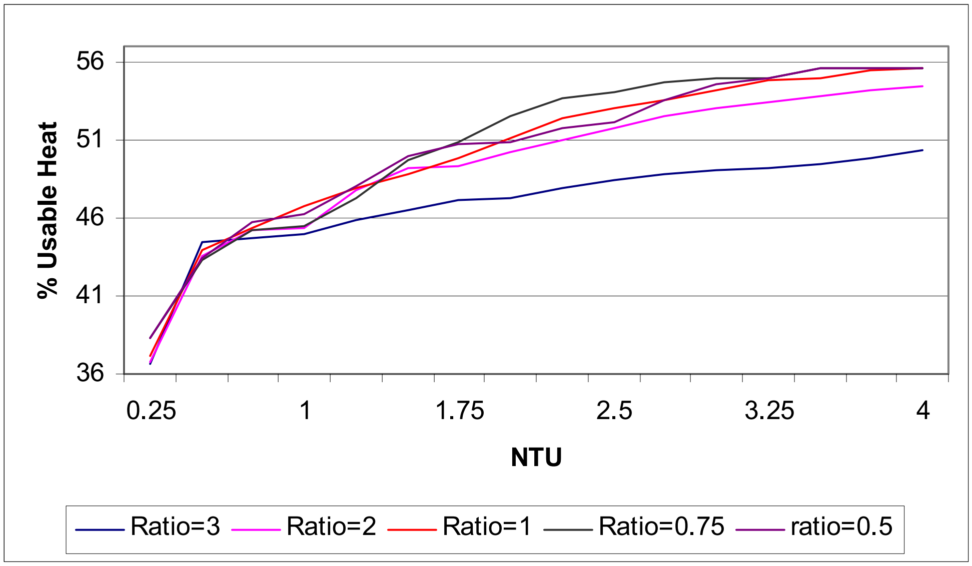

Figure 5.5 NTU vs. % Usable Heat for Hot Side Flow Rate of 1500 kg/hr

The maximum amount of usable heat is between 45-49 % and 55-56 % for hot side flow rates between 250-500 kg/hr and 1000-1500 kg/hr respectively. The maximum occurs for all flow rates at an NTU of about 4. The results show a significant reduction in the usable heat for lower flow rates of 250-500 kg/hr, compared to higher flow rates of 1000-1500 kg/hr. Analyzing the higher flow rates, it can be seen that the percentage of usable heat remains fairly consistent for NTU values greater than 2.5 and 3.25 for 1000 kg/hr and 1500 kg/hr flow rates. This indicates that higher UA values of the heat exchanger will not provide an additional heat transfer to the cold-water flow, which will allow for the design of a smaller and less expensive heat exchanger.

The design of the optimal ratio of the fuel cell capacitance rate to the storage capacitance rate may be determined by investigated the maximum usable heat at the given NTU value. Comparing figures 5.4 and 5.5 it can be seen that at a flow rate of 1000 kg/hr and NTU value of 2.5 the percentage of usable heat is 55 at an ratio of 1.0, while for a flow rate of 1500 kg/hr and a NTU of 3.25 the percentage of usable heat is 55 at an ratio of 0.5. Therefore this analysis as shows that 1000 kg/hr for a hot side flow rate will provide a maximum and most economical flow rate for the heat exchanger.

The heat exchanger analysis has determined that a flow rate of 1000 kg/hr will be used for the fuel cell collector and storage side of a heat exchanger with an NTU value of 2.5, which yields a UA value of 5239 kJ/hr-K.

5.2.3 Thermal Storage Tank

The thermal storage tank is one of the critical components of the system because it stores the rejected waste heat from the fuel cell system contributes to the usable water and space heating applications. The losses from the storage tank are very important and will help determine the optimal size for fuel cell system. Figure 4.24 determined the stratification of the tank and the optimal number of nodes, and the tank will consist of 20 nodes. The storage tanks will be located within a basement or crawl space and the environmental temperature of the surroundings is determined by equation 4.28. Analyzing Figures 5.6 and Figure 5.7 will determine the optimal size of the storage tank.

Figure 5.6 examines the affect of changing the storage tank size for the main storage tank. It can be seen that the optimal size of the tank will be an 80-gallon tank. The smaller tanks will not provide adequate heating for water heating, and will present the lowest amount of the thermal heat utilized. Increasing the storage tank above 80-gallons will reduce the amount of thermal heat utilized and this is due to the large thermal losses associated with the increasing storage size.

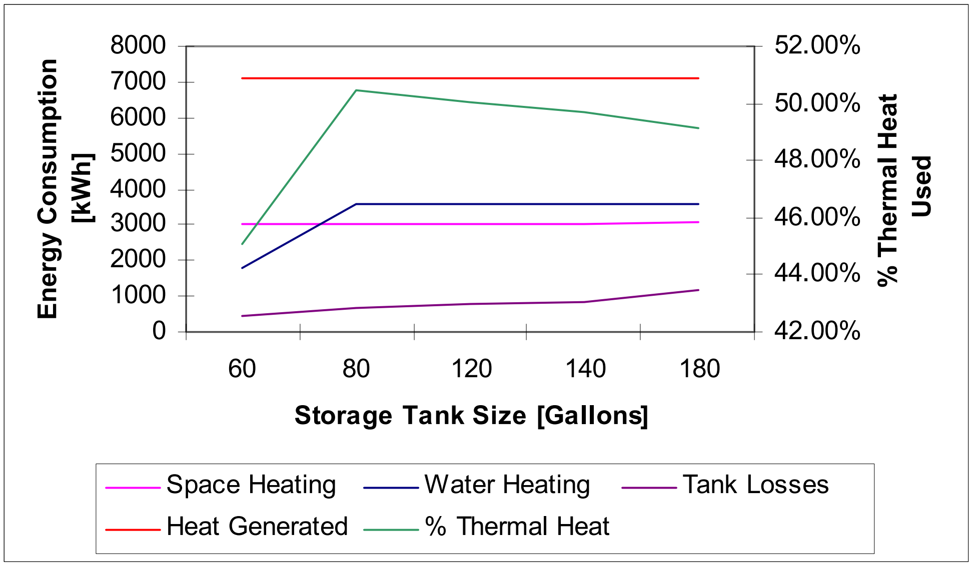

Figure 5.6 Main Thermal Storage Tank Effects

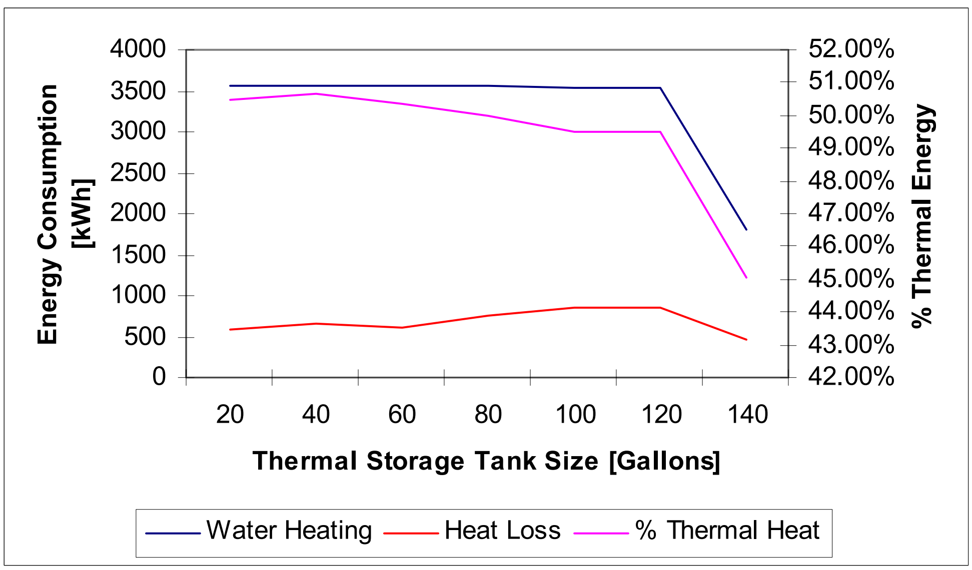

Figure 5.7 Domestic Hot Water Storage Tank

Figure 5.7 examines the domestic hot water storage tank. The maximum thermal energy utilized will be with a 40-gallon storage tank. Increasing the storage tank size will not provide an added benefit to the system; it will only increase the thermal losses and therefore reducing the overall thermal energy utilized. The smaller tank will not provide an adequate amount of storage for the hot water demand and therefore will require auxiliary energy, which will reduce the overall thermal energy utilized.

5.2.4 Fuel Cell System Performance

The combined heat and power fuel cell system will run to supply the residential lights, appliances and space cooling loads. The system will operate with a 1.5 kW rated fuel cell stack, 80-gallon storage tank, 40-gallon hot water tank, and an NTU value of 2.5 for the storage side heat exchanger. The PEM fuel cell system is designed to instantaneously respond to the partial load operation experienced by the residence. The partial load is defined as the electrical demand of the house over the maximum rated capacity of the fuel cell, in this case 1.5 kW. Figure 5.8 details a 3-day operation of the power demands of the fuel cell system. It is shown that for a typical household with a varying partial load the fuel cell system can control the system. The PEM fuel cell system will provide 96% of the residences electrical demand. Figure 5.9 details the part load ratio of the fuel cell system. This figure will allow for a general determination of the system efficiency and the thermal heat generated from a fuel cell system, based on the varying electrical demand. The thermal heat is determined by the thermal-to-electric ratio, and the system efficiency is based on ratings of 75%, 80%, and 70% respectively for the reformer, fuel utilization, and power conditioning equipment.

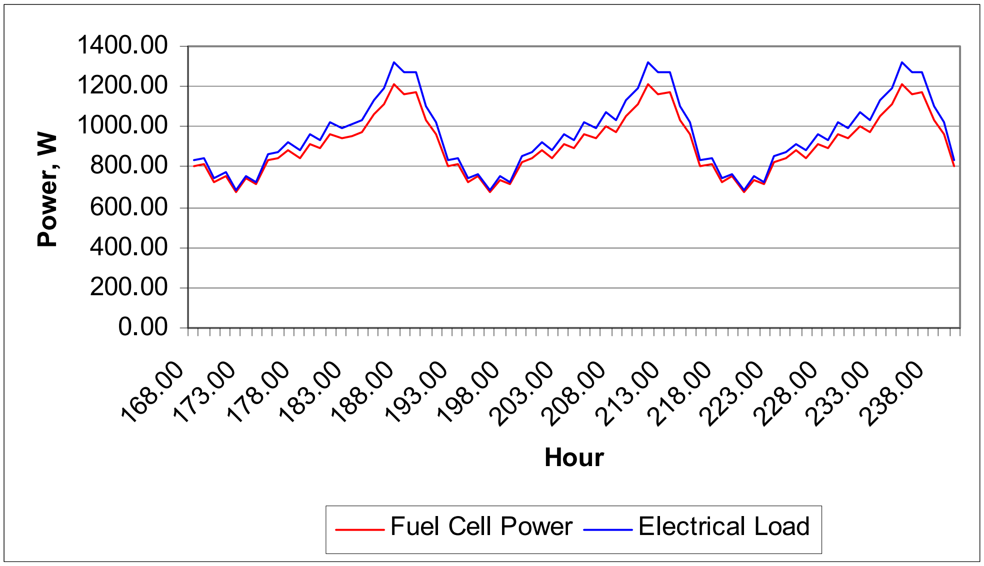

Figure 5.8 Residential Power Demand and Power Supply from the Fuel Cell System

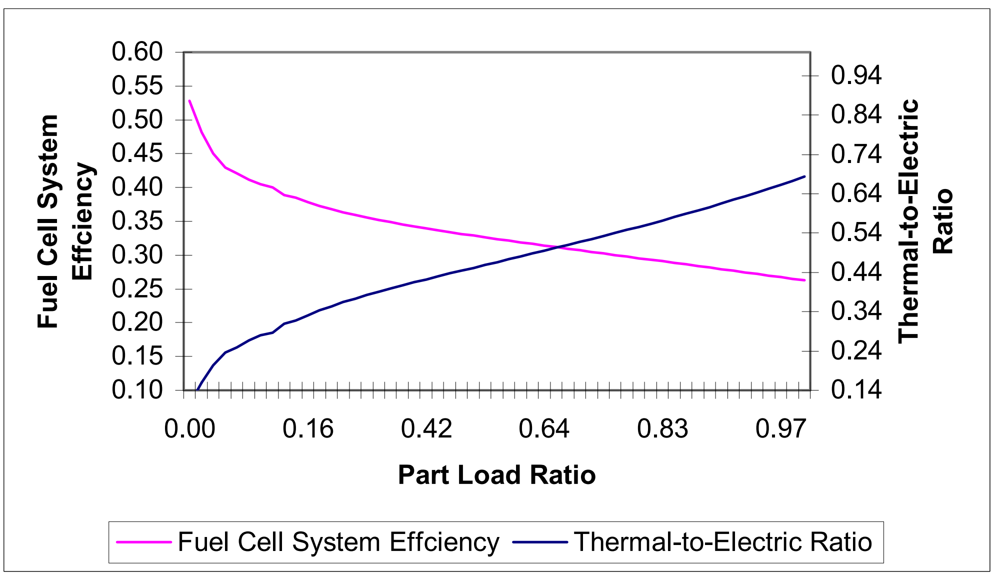

Figure 5.9 Thermal and Electric Efficiencies for Various Part Loads

The thermal heat from the fuel cell system will provide approximately 50-55 % of the total thermal loads of the residences located in the colder climates and 65-70 % of the total thermal loads of the residences located in the warmer climates. The desired hot water temperature of the residence is 60^0 C, and the storage tank is not allowed to fall below 55^0 C. The total water heating loads for both locations will be provided by the fuel cell system.

Figure 5.9 shows the storage tank temperature over a typical month, for the location in Boston. It is shown that the storage tank temperature does not fall below the minimum requirement.

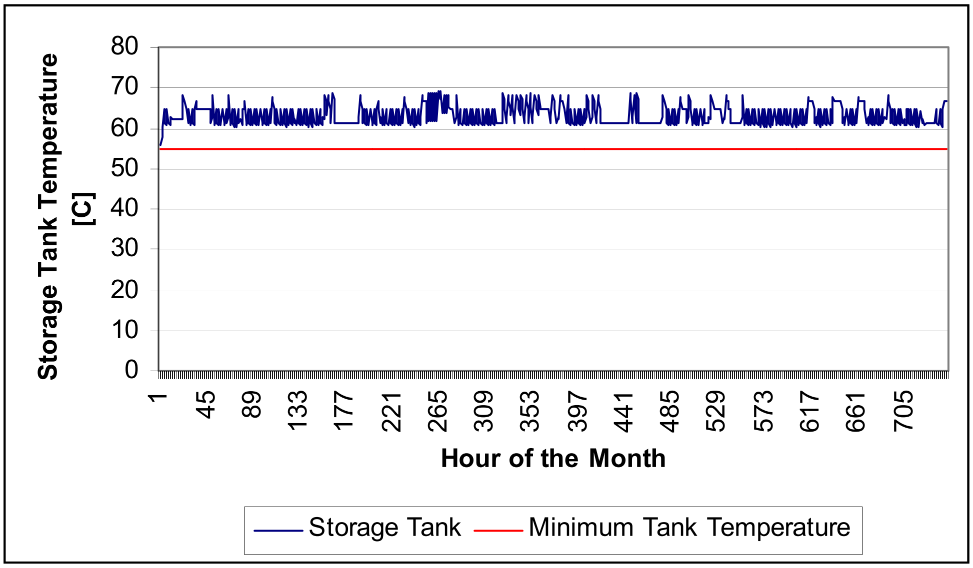

Figure 5.10 Storage Tank Temperatures for a Typical Month

5.3 Energy Characteristics

The following section will determine the energy characteristics for the combined heat and power fuel cell system. The section will look at the amount of energy required for the fuel cell system and the auxiliary energy required for each system, and compares the different systems to conventional systems.

5.3.1 End-Use Energy

The annual energy required for operation the fuel cell system with the auxiliary systems for the colder climate, Boston, and the warmer climate, Atlanta, are presented in Figures 5.11 and 5.12. The thermal storage tank losses are very negligible compared to the unavailable energy and the heat rejection. The unavailable energy is the amount of energy that will be rejected by the fuel cell system into the environment and for Atlanta, 24% and Boston, 19% of the energy inputted to the CHP system is rejected into the environment. The heat rejected from the system is determined by how much of the recovered heat is not utilized during the annual operation. In Boston only 3% of the collected heat is rejected, while in Atlanta 7% is rejected. The increase for Atlanta can be attributed to the longer cooling season compared to the heating season of Boston. The percentage of each of the residential end-uses compared to the input energy for the system may also be recognized within the Figures.

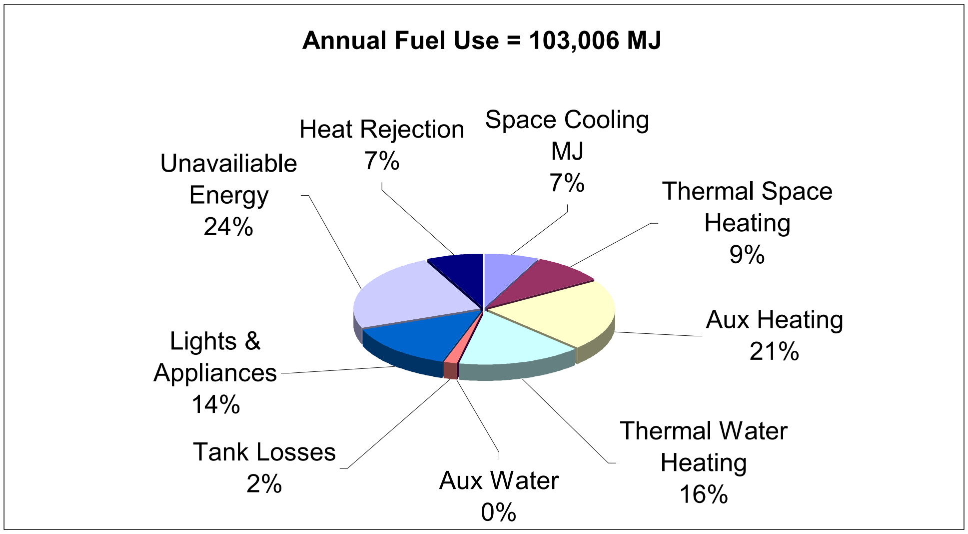

Figure 5.11 Fuel Utilization, Atlanta GA

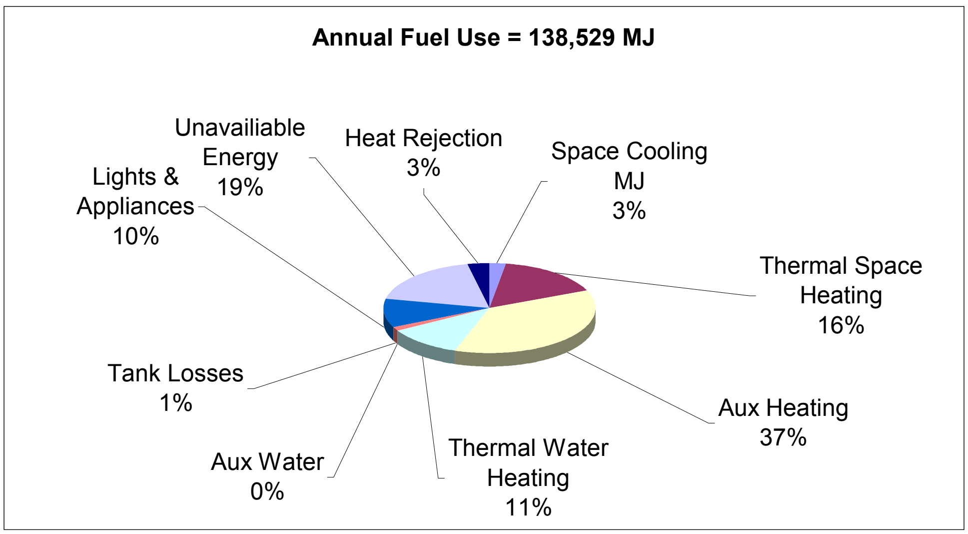

Figure 5.12 Fuel Utilization, Boston, MA

Figures 5.11 and 5.12 presented the energy end-use for a fuel cell system operating based on the residential lights, appliances, and space cooling demands. Figures 5.13 and 5.14 present the energy end-use for a fuel cell system sized to operate at a constant 1.5 kW output. The system is designed continuously supply 1.5 kW output which will supply the space cooling, lights, and appliance loads, but also the system will produce an added amount of heat for water heating and space heating, while producing an excess amount of electricity that will be used for an added space heating, and electricity to be sold back to the electric grid. Operating the fuel cell system at a constant electrical production greatly increases the fuel use for each location, but provides the reduction of the amount of auxiliary energy needed. It is shown that the system will provide over 30% and 40% of the space heating demand in Atlanta and Boston respectively. The amount of space heating is greater in Boston due to the colder climate, and the thermal heat is better utilized than in Boston, this reasoning may also be supported by the fact that 3% of the recovered heat is rejected in Boston compared to 10% for Atlanta.

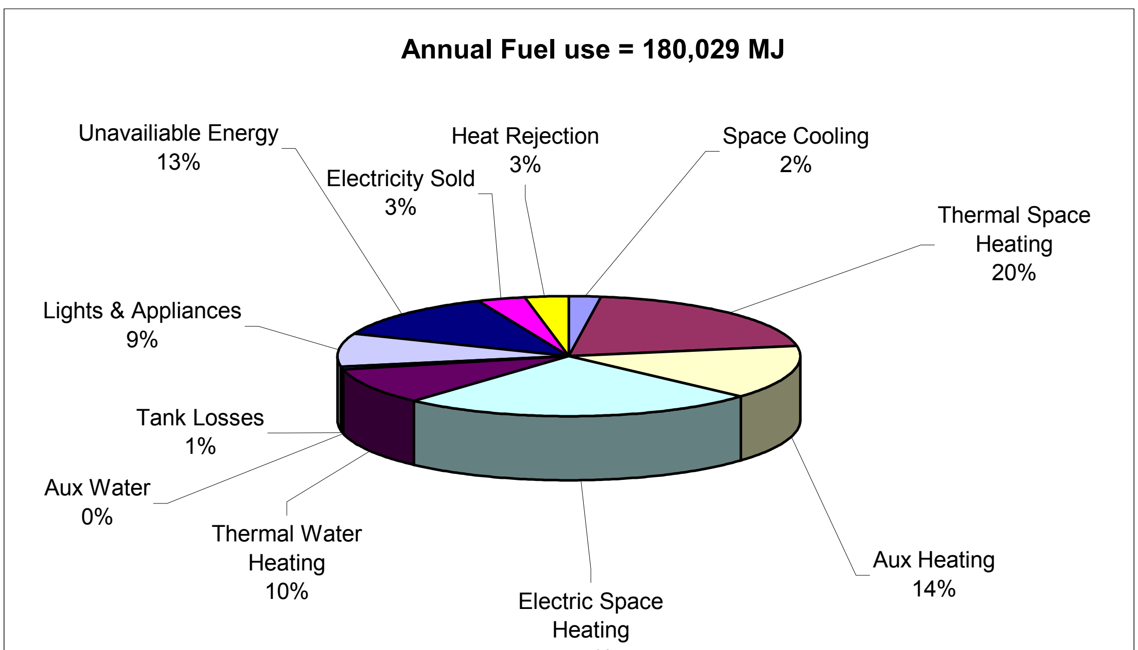

Figure 5.13 Fuel Utilization, Boston, MA For Constant 1.5 kW

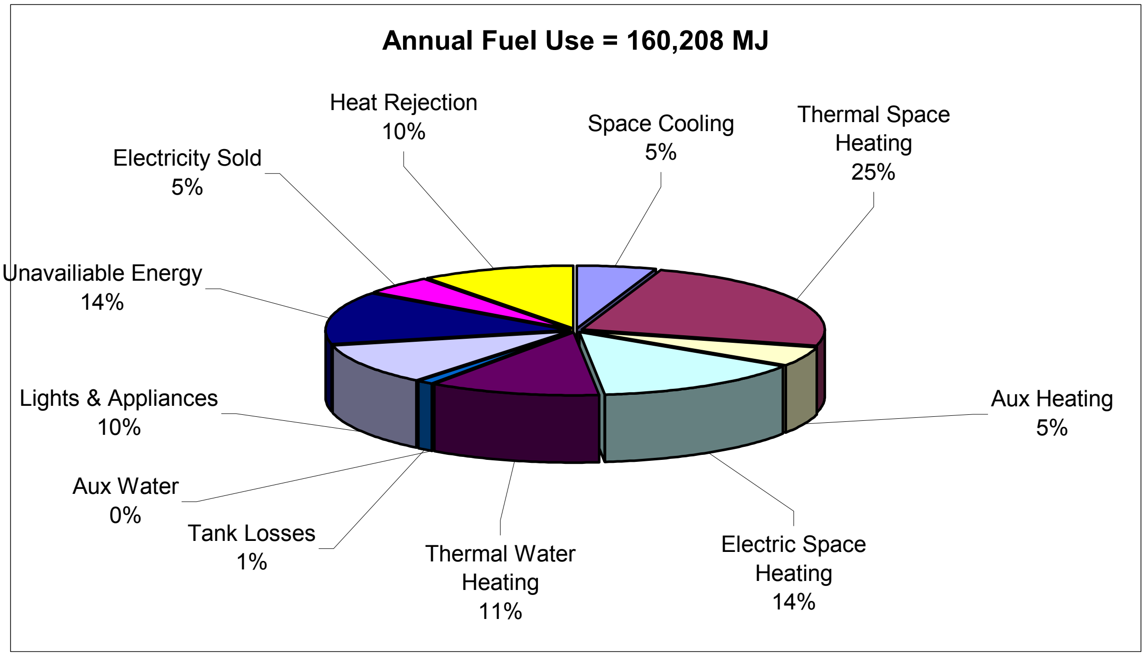

Figure 5.14 Fuel Utilization, Atlanta, GA for Constant 1.5kW

The cogeneration efficiencies of the systems will be determined by taking the sum of the electrical and thermal production from the fuel cell system over the annual fuel use of the system. The system operating under the desired load will have cogeneration efficiencies of 54% and 40% for the locations in Atlanta and Boston respectively. The systems that will operate under a constant 1.5 kW load will have efficiencies of 67% and 60% for those cities. The increase in the cogeneration efficiencies is directly related to the reduction in amount space heating required, and even though the thermal heat is better utilized in the colder climates the high heating demand still requires an abundant amount of auxiliary space heating.

5.3.2 Energy Savings

The combined heat and power fuel cell system, is designed to reduce the amount of energy required to supply residential energy demands. Table 5.12 provides the total amount of energy inputted into the CHP system and the energy savings compared to the

Table 5.12 Energy Savings Comparison

Table 5.12 Energy Savings Comparison				
CHP vs. Conventional Systems				
	Boston	Chicago	Atlanta	Sacramento
All Electric System [MJ]	207,729	219,935	170,364	168,476
Electric and Natural Gas System [MJ]	188,304	201,878	139,669	137,748
Combined Heat and Power System [MJ]	138,529	142,708	103,006	102,023
% Energy Saving vs. All Electric	33%	35%	40%	39%
% Energy Savings vs. Electric and Natural Gas	26.43%	29.31%	26.25%	25.93%
1.5 kW vs. Conventional Systems				
	Boston	Chicago	Atlanta	Sacramento
All Electric System [MJ]	207,729	219,935	170,364	168,476
Electric and Natural Gas System [MJ]	188,304	201,878	139,669	137,748
Combined Heat and Power System [MJ]	180029	201097	160208	157694
% Energy Saving vs. All Electric	13%	9%	6%	6%
% Energy Savings vs. Electric and Natural Gas	4.39%	8.57%	5.96%	6.40%

conventional systems energy input. The energy savings for the system operating under the instantaneous residential load provides excellent energy savings for all locations. Conventional all electric systems can see savings of 30-40%, while the conventional electric and natural gas systems may see savings of 25-30%. The system operating at a constant 1.5 kW will have an energy savings from 6-13% compared to conventional all electric systems. Compared to an electric/natural gas conventional system, the continuous 1.5 kW systems will have savings from 4-8%. The main advantage with the operation of a fuel cell system operating at constant load would be the potential savings in the amount of electricity being sold back to the electric grid, which will be analyzed in the following section.

5.4 Economic Analysis

The cost of electricity has been evaluated, and as expected it has a linear relationship with respect to the cost of the fuel cell itself. (Figure 5.15)

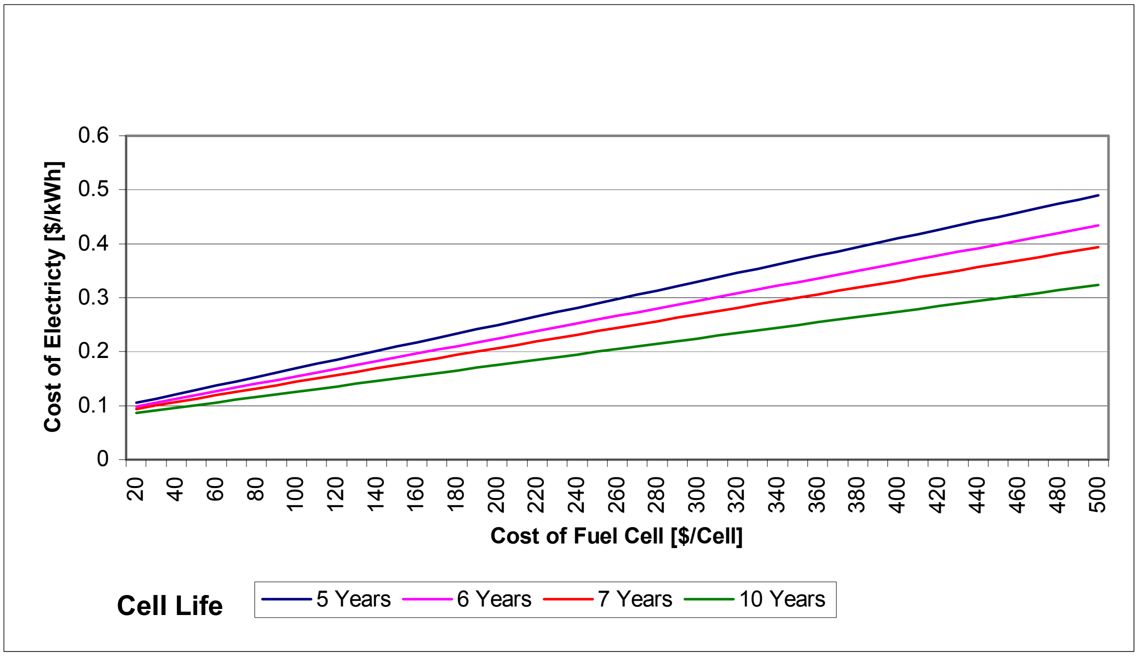

Figure 5.15 Comparison of Cost of Fuel Cell vs. Cost of Electricity

Figure 5.15 was developed with the assumption that the fuel cell will operate at 50% efficiency and a part load ratio of 0.6. Improving the life of the fuel cell will also improve the cost of electricity. Fuel cell stack life span is estimated at 5 years, improving that life span to 10 years will drastically decrease the cost of electricity, for a fuel cell stack cost of $500/ stack the cost of electricity will decrease by 0.158 $/kWh.

The life cycle analysis will consist of four major life cycle calculations: the initial cost of the CHP system, maintenance cost of the system, energy costs, and the cost of electricity sold back. The initial cost and maintenance cost of the CHP is determined by the values in Table 4.72. First evaluating the cost of electricity for the fuel cell system, and looking at the energy requirements for the fuel cell system and also the auxiliary energy requirements will determine the energy cost. The life cycle analysis will run on a 20-year life span and the cost for natural gas and electricity are presented in Table 4.71. Figures 5.15 and 5.16 provide the life cycle savings of the fuel cell system compared to all electric and natural gas-electric systems.

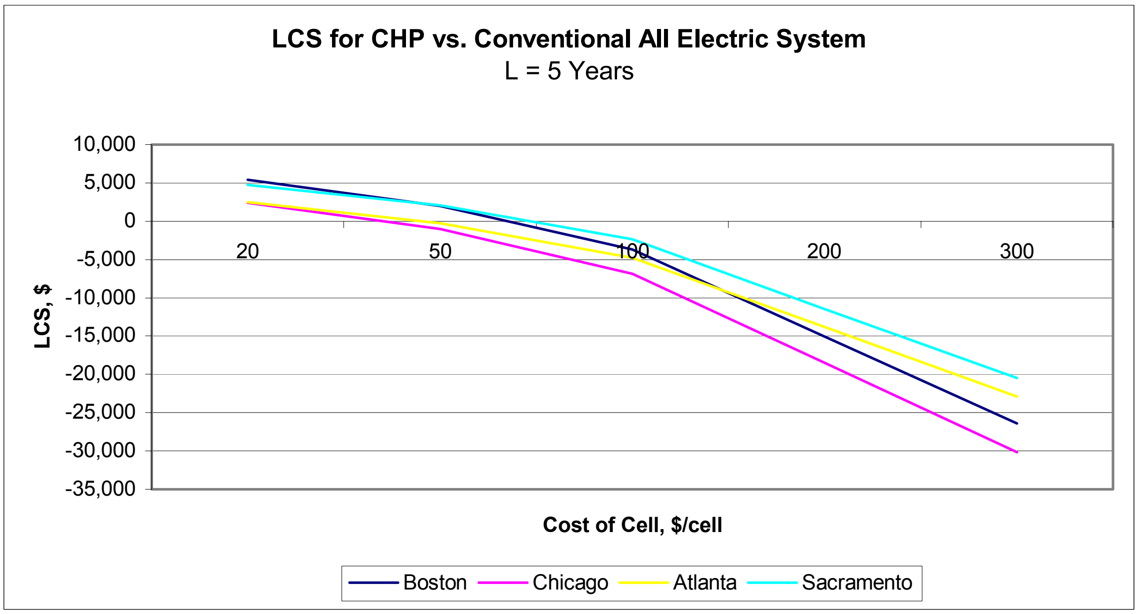

Figure 5.16 Comparisons of Life Cycle Savings vs. All-Electric System

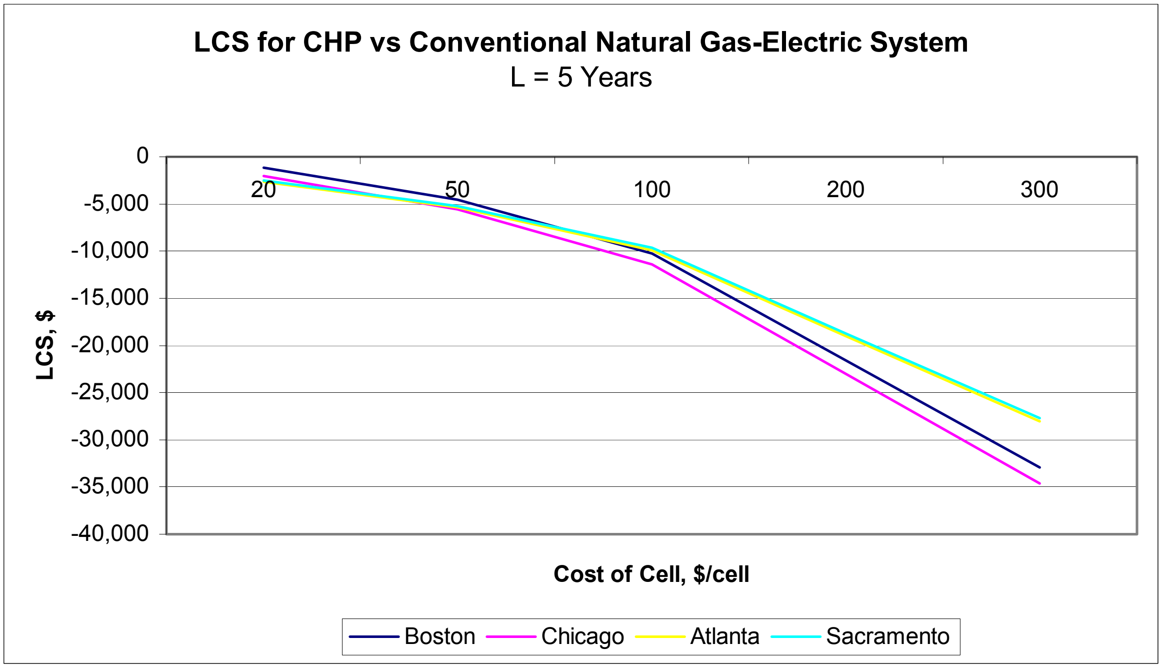

Figure 5.17 Comparison of Life Cycle Savings vs. Natural Gas-Electric System

It is evident that in the current marketplace for fuel cells are extremely high for all locations compared to conventional systems. In order for fuel cells to become economically variable, their life cycle savings compared to conventional systems must reach a zero difference, for an all-electric system the fuel cell itself must reach a price of $75/cell and $40/cell for the southern and northern climates respectively. The fuel cell must reach a price of under $20/cell for all locations in order for the fuel cell system to become competitive against a natural gas-electric system. The results for Figures 5.14 and 5.15 assumed that the life of the fuel cell stack is only five years, improving the stack life will improve the LCS as seen in Figures 5.18 and 5.19:

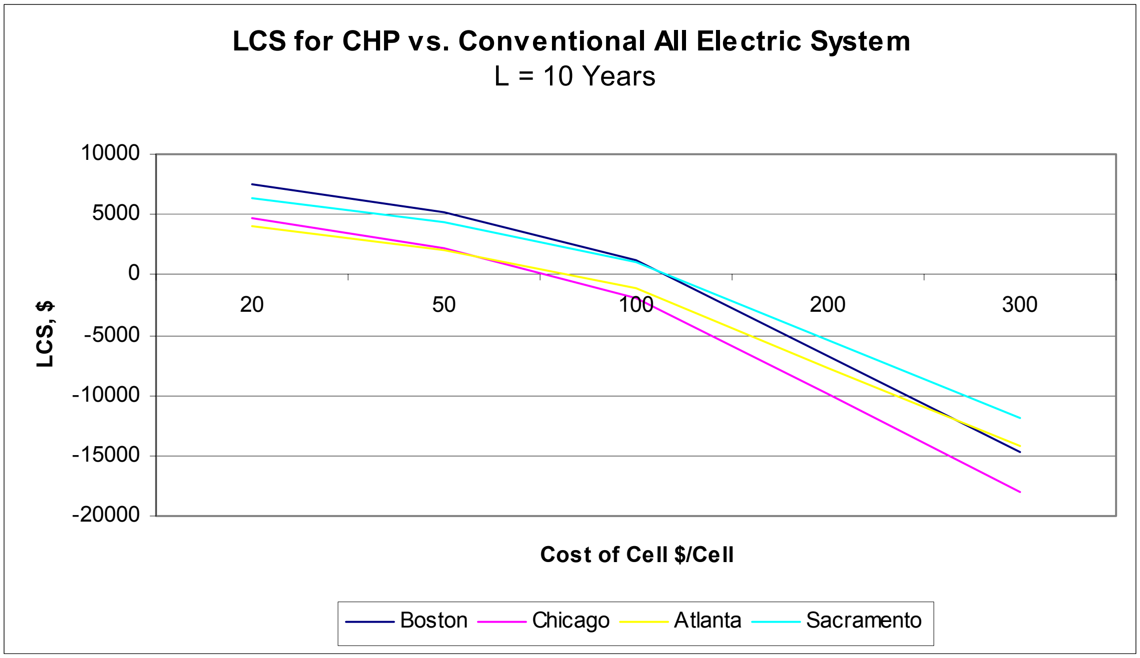

Figure 5.18 Comparison of LCS vs. All-Electric System with a Stack life of 10 Years

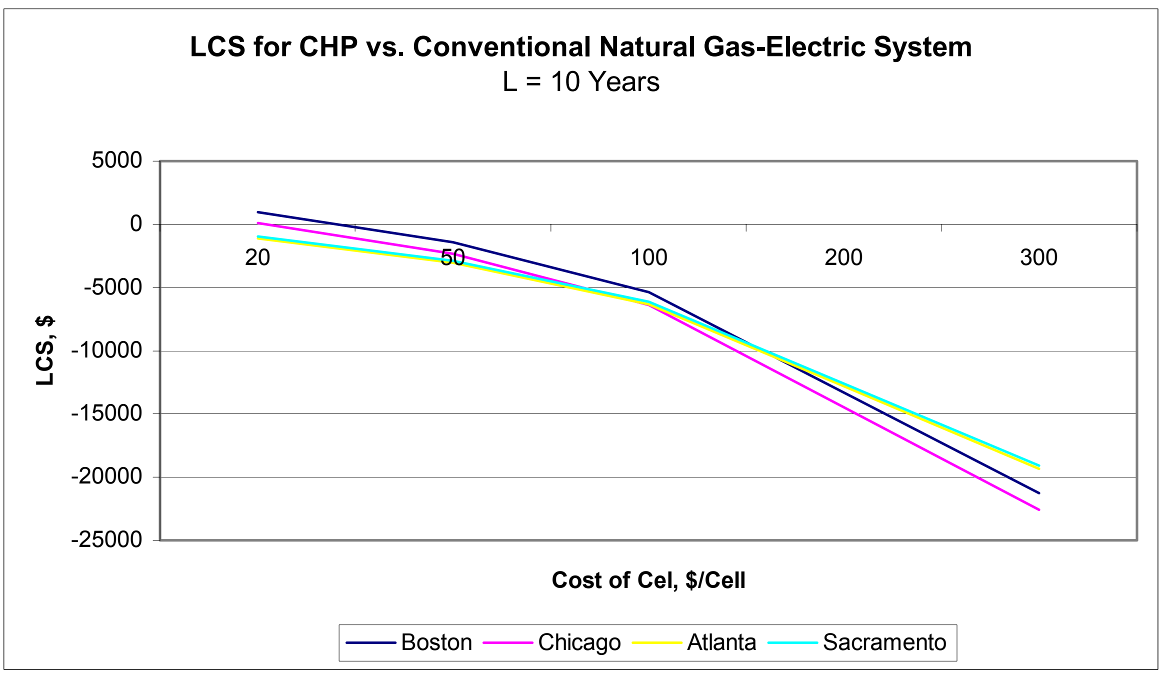

Figure 5.19 Comparison of LCS vs. Natural Gas System with a Stack life of 10 Years

It can be seen from the figures that improving the stack life shows that an all-electric system, the price of each fuel cell needs to become $75/cell and $105/cell for the northern and southern climates respectively, for the life cycle savings to be competitive. Comparing the natural gas-electric conventional system the stack life does not have a major effect on the life cycle savings; the price of the cell still needs to be in the order of $20.

5.5 Conclusion

This research has investigated the possibility of implementing a combined heat and power fuel cell system for various locations within the United States, and has found that the possibility can be an alternative solution to conventional residential energy supplies. This chapter will summarize the design consideration for the CHP system.

The fuel cell system has been sized to accommodate the average peak electrical demand for a cooling day, neglecting power surges; an average of 1.0 and 1.5 kW may be used for both the northern and southern climates respectively.

The heat exchanger that captures the generated heat from the fuel cell stack and provides the thermal energy needed for heating loads, with a NTU value of 2.5 and hot side flow rate of 1000 kg/hr as shown to be the most economical heat exchanger available. Increasing the UA value and the flow rate will not provide additional heat transfer, and decreasing the parameters will reduce the amount of thermal heat captured from the fuel cell stack.
The main hot water storage tank will be sized at 80-gallons, and the hot water tank will be sized at 40-gallons. The sizing of the tanks will provide the full hot water demand for all

residences, while reducing the thermal losses from the tanks, which will increase the efficiency of the total system.

The fuel cell system will provide approximately 96% percent of the electrical demand for all households resulting in cogeneration efficiencies of 40% for the northern climates and 58% for the warmer climates. This indicates that the fuel cell system with a dual storage tank system is a good match for responding to the residential electrical and heating demands, if the fuel cell system where to run on a continuous 1.5 kW output the cogeneration efficiency for the northern climates will raise to 65% while for the warmer climates the cogeneration efficiency drops to 56%.

The current price of fuel cells will not provide an added benefit for the implementation of a fuel cell system compared to either an all-electric system or a natural gas-electric system. Compared to an all-electric system the price of the fuel cell with reformer needs to be manufactured to at least $40/cell and $75/cell for the northern and southern climates respectively, for a system compared to a natural gas-electric conventional system the manufacturing costs need to be made under $20/cell for all locations.

5.6 Final Remarks

This thesis has attempted to model the performance of a Proton Exchange Membrane Fuel Cell System for various climatic conditions. It is my conclusion that in the northern climates a 1.5 kW system running continuously, and a 1.5 kW system running based on the residential demand will provide the most optimal and economical design for a fuel cell system.

Bibliography:

1. Energy Information Administration (EIA) *http://www.eia.doe.gov/*

2. A Transient System Simulation Program (TRNSYS), Solar Engineering Laboratory, University of Wisconsin-Madison, WI, 2002 *http://sel.me.wisc.edu/trnsys/*

3. United States Combined Heat and Power Association, "CHP Recourses" http://www.nemw.org/uschpa/index.html

4. The European Association for the Promotion of Cogeneration, "A Guide to Cogeneration" www.cogen.com, 2001

5. A. J. Appleby, F.R. Foulkes, "Fuel Cell handbook", Krieger Publishing Company, 1993

6. J. Bockris, "Fuel Cells: Their Electrochemistry" McGraw-Hill, 1968

7. Larmine, James, Fuel Cell Systems Explained, John Wiley 2000

8. Gunes, M.B, "Investigation of a Fuel Cell Based Total Energy System for Residential Applications" M.S. Thesis Department of Mechanical Engineering, Virginia Polytechnic Institute and State University, 2001

9. Krist, K, Gleason, K, Wright, J, "SOFC-based Residential Cogeneration Systems" *Electrochemical Society*, (1999), 107-15

10. Bos, P.B, "Commercializing Fuel Cells: Managing Risks" *Journal of Power Sources* 61 (1996) 21-31

11. Braun, R.J, "Optimal Design and Operation of Solid Oxide Fuel Cell Systems for Small-scale Stationary Applications" Ph.D. Dissertation, Department of Mechanical Engineering, University of Wisconsin-Madison, 2002

12. Leo J, M. J. Blomen, M.N. Mugerwa, Fuel Cell Systems, 1993 Plenum Press, NY

13. B.R. Becker, K.E. Stogsdill, Development of a Hot Water Database, *ASHRAE Transactions*, 1990 Part2 V96

14. A. Lowenstein, C. Hiller "Disaggregating Residential Hot Water Use- Part I, *ASHRAE Transactions* 1998 Part1B 1853-1863

15. W. DeOreo, P. Mayer, "The End Uses of Hot Water In Single Family Homes From Flow Trace Analysis" Aquacraft, Inc Water Engineering and Management, 2001

16. ASHRAE "Handbook of Fundamentals" 1993

17. Charles Eley, "Residential Water Heating Hourly Calculations", Controlled Energy Corporation, 2002

18. Duffie, J.A, Beckman, W.A. "Solar Engineering of Thermal Processes" John Wiley & Sons, 1991

19. F. Johnson, R. Brown, J Hanford, A. Sanstad, J. Koomey*;* "Residential HVAC, Assumptions and Methodology for End-Use Forecasting with EPRI-REEPS 2.1"; June 1994 Lawrence Berkeley Laboratory University of California Berkeley

20. Arasteh, D. Huang, J. Mitchell, R. Clear, B. Kohler, C. (1999) "A Database of Window Annual Energy Use in Typical North American Single Family Houses" *ASHRAE Transactions, 106*

21. National Association of Home Builders, "Review of Residential Electrical Energy Use Data" NAHB Research Center, Inc, 2001

22. A. Heinzel, B. Vogel, P. Hubner, "Reforming of Natural Gas-hydrogen Generation for Small Scale Stationary Fuel Cell Systems" *Journal of Power Sources*, 105 (2002), 202-207

23. Hydrogems Energy Models, "Type170; Proton Exchange Membrane Fuel Cell" http://www.hydrogems.no/, 2002

24. C. Berger, "Handbook of Fuel Cell Technology", Prentice Hall, Engelwood Cliffs, NJ, 1968

25. O. Ullerberg, "Stand Alone Power Systems for the Future: optimal Design, Operation & Control of Solar-Hydrogen Energy Systems" Ph.D. Dissertation, Department of Thermal Energy and Hydropower Norwegian University of Science and Technology, 1998

26. J.C. Amphlett, R.F. Mann, B.A. Peppley, P.R. Rpberge, A. Rodrigues, “A Model Predicting Transient Responses of Proton Exchange Membrane Fuel Cells” *Journal of Power Sources* 61 (1996) 183-188

27. H. Laukamp, “Inverter for Photovoltaic Systems” Fraunhofer Institute for Solar Energy system, Freiburg im Breisgau, Germany

28. F. Incropera, D. DeWitt, “Fundamentals of Heat and Mass Transfer” John Wiley and Sons, 2002

29. Barbir, F, Gomez, T “Efficiency and Economics of Proton Exchange Membrane Fuel Cells” *International Journal of Hydrogen Energy*, Volume 21, Issue 10, October 1996, Pages 891-901

30. Bar-On, I, Kirchain, R, Roth,R “Technical Cost Analysis for PEM Fuel Cells” *Journal of Power Sources*, Volume 109, 2002 Pages 71-75

31. Grainger Industrial and Commercial Equipment and Supplies Catalog No. 386, http://www.grainger.com, 2002